

Magnetic Resonance Spectroscopy of the Human Brain

BRIAN ROSS* AND STEFAN BLUML

Magnetic resonance (MR; synonymous with NMR = nuclear magnetic resonance) is a universal physical technique best known for non-invasive detection and anatomical mapping of water protons (H). MR-spectroscopy (MRS) records protons from tissue chemicals other than water, intrinsic phosphorus containing metabolites, sodium, potassium, carbon, nitrogen, and fluorine. MRS is therefore an imaging technique with the potential to record human and animal biochemistry in vivo. As a result of wide availability of MRI equipment in research laboratories and hospitals, MRS is a serious competitor with PET to define normal body composition and its perturbation by pharmacological and pathological events. This article describes practical aspects of in vivo MRS with particular emphasis on the brain, where novel metabolites have been described. A survey of these new aspects of neurochemistry emphasize their practical utility as neuronal and axonal markers, measures of energy status, membrane constituents, and osmolytes, as well as some xenobiotics, such as alcohol. The concept of multinuclear in vivo MRS is illustrated by diagnosis and therapeutic monitoring of several human brain disorders. Although these methods are currently most frequently encountered in human studies, as well as with transgenic and knockout mouse models, MRS adds a new dimension to anatomic and histopathologic descriptions. *Anat Rec (New Anat)* 265:54–84, 2001. © 2001 Wiley-Liss, Inc.

KEY WORDS: biomedical imaging; magnetic resonance imaging; MRI; MRS; spectroscopy; neurochemistry; brain disease; N-acetyl aspartate; myelination; Canavan disease; Huntington disease; Alzheimer disease

Twenty years ago, the optimum techniques available to address a metabolic question in the brain were considered to be, in order of reliability: brain slices in vitro, arterio-venous

difference in vivo across the jugular bulb and carotid artery, isolated intact brain perfusion in situ and, the then newly emerging techniques of isolated brain-cell preparation (Ross, 1979). Almost at the same time, however, there appeared a seminal paper describing the transfer, after 25 years, of the chemists' major investigational tool, nuclear magnetic resonance spectroscopy (MRS; see Box 1 for a complete list of abbreviations), to the intact mammalian brain in vivo (Thulborn et al., 1981). Soon thereafter followed in vivo MRS of human muscle (Ross et al., 1981), and of neonatal (Hamilton et al., 1986) and adult human brain (Bottomley et al., 1983).

Today, few university hospitals in the world are without a whole-body MR scanner capable of assaying metabolites non-invasively in the human brain, using robust MRS methods. Together with MRS, physiological MRI, fMRI, and PET, the neuroscientist can now reverse the order of preference

when considering a technique with which to address a metabolic question in the brain. It is almost certainly "easiest" to turn first to the intact human brain with in vivo magnetic resonance spectroscopy. How best to do this in practice is the subject of this article.

As a spectroscopy technique, the product of MRS is a printout of peaks of different radio-frequency and intensity, recording molecules that possess the intrinsic property of the NMR technique, nuclear spins, unique resonance frequencies, spin-couplings, and relaxation properties. Many classical neurochemical events are readily documented in the human brain in vivo through MRS. But the molecules that yield the optimum MR-signals are not always those of which the neuroscientist first thinks, or even wants, in her or his pre-conceived experiment. As a result, in the first 20 years of in vivo brain MRS, some "new" neurometabolites have come to the fore.

Dr. Ross, a physician and neurologist [MD/DPhil(Oxon)], trained at the University of Oxford, UK. He is the Director of the Clinical MR Unit at Huntington Medical Research Institutes (HMRI) in Pasadena, CA; Professor of Clinical Medicine at the University of Southern California School of Medicine in Los Angeles; and Visiting Associate, Chemistry and Chemical Engineering at Caltech in Pasadena. Dr. Bluml received his PhD training in physics at the universities of Freiburg and Heidelberg, Germany. Currently he is senior physicist in the Clinical MR Unit at HMRI, Director of Research for Rudi Schulte Research Institutes in Santa Barbara, CA, and was recently appointed Associate Professor in Radiology at USC. Grant sponsor: Rudi Schulte Research Institute; Grant sponsor: NIH; Grant sponsor: HMRI.

*Correspondence to: Dr. Brian Ross, Clinical Magnetic Resonance Spectroscopy Unit, Huntington Medical Research Institute, 660 South Fair Oaks Avenue, Pasadena, CA 91105. Fax: (626)397-5889. E-mail: soccss@hmri.org

Box 1. Abbreviations Used in Magnetic Resonance Imaging and Spectroscopy

MRI, magnetic resonance imaging; MRS, magnetic resonance spectroscopy; PET, positron emission tomography; SPECT, single photon emission computed tomography; fMRI, functional MRI; MS, multiple sclerosis; AD, Alzheimer dementia; ALD, adrenoleukodystrophy; STEAM, stimulated echo acquisition mode; PRESS, point resolved spectroscopy; ISIS, image selected in vivo spec-

troscopy; CSI, chemical shift imaging; VOI, volume of interest; NAA, *N*-acetylaspartate; Cr, creatinine; ml, *myo*-inositol; Cho, choline; PCr, phosphocreatine; GPC, glycerophosphocholine; GPE, glycerophosphoethanolamine; PC, phosphocholine; Glx, glutamine; glu, glutamate.

PRINCIPLES OF NEUROSPECTROSCOPY

We define neurospectroscopy as the field of study resulting from MRS examination of the human brain. Diseases and pathologies of the brain are commonly classified as:

- structural (including degenerative, tumor and embryogenic defects);
- physiological (essentially interruption of blood supply); and
- biochemical or genetic.

Of the latter, some are receptor and neurotransmitter-related (e.g., dopa-

Today, few university hospitals in the world are without a whole-body MR scanner capable of assaying metabolites non-invasively in the human brain, using robust MRS methods.

mine in Parkinson disease) but many are directly or indirectly related to disturbances of the pathways of oxidative, anabolic and catabolic intermediary metabolism, the tricarboxylic acid (TCA) or Krebs cycle, glutamine/glutamate turnover, glycolysis, ketogenesis or fatty acid metabolism. PET, and to a lesser extent SPECT (see Figure 1), MRI, fMRI and diffusion-imaging address blood flow, glucose turnover and oxygen consumption, and PET and SPECT are uniquely able to “image” targeted receptor ligands. Until the advent of NMR, however, no

TABLE 1. Current methods of magnetic resonance spectroscopy available for the brain

Clinical Method	Rf Coil Available	Implementation on Clinical 1.5T
Localized ¹ H MRS		
Long echo	*	*
Short echo	*	*
Quantitation	*	*
Phase-encoded imaging of metabolites, CSI	*	*
Fast metabolite imaging	*	*
Automation	*	*
Osmolality	*	*
Editing	*	*
Functional MRS	*	*
Localized ³¹ P MRS		
Pulse-acquire		*
Decoupled ¹ H- ³¹ P		*
Phase-encoded imaging, CSI	*	*
Fast phosphocreatine imaging	*	*
Magnetization transfer (flux)		*
Localized ¹³ C MRS		
Natural abundance	*	*
¹³ C enriched-flux measures	*	*
¹ H- ¹³ C heteronuclear methods	*	*
Localized ¹⁵ N MRS		
¹⁵ N enriched-flux measures		
¹ H- ¹⁵ N heteronuclear method(s)		
Localized ¹⁹ F MRS		
¹⁹ F drug detection		
¹⁹ F imaging and blood flow methods	*	*
(¹⁹ F probes for Ca ²⁺ and Mg ²⁺ = determination) ^a		*
⁷ Li MRS		
²³ Na MRS		

^aToxic in vivo.

direct non-invasive assay of the products of gene expression, the cerebral metabolites, was available. There was no neuronal marker, no astrocyte marker and no technique to directly determine energy metabolism. These gaps are now filled by neurospectroscopy and, with increased clinical experience, a diagnostic "need" for magnetic resonance spectroscopy (MRS) of the brain emerges.

METHODS FOR HUMAN NEUROSCPECTROSCOPY

At least 20 methods are available for human neurospectroscopy. Table 1 outlines the currently available methods of MRS as applied to the brain. The first applications of MRS with surface coils demonstrated the potential of MRS for non-invasive insights into brain metabolism (Ackerman et al., 1980). The lack of a proper localization, using this easy and straightforward technique, has been partly overcome by improvements (Bottomley et al., 1984). In the clinical setting of neurospectroscopy, however, more advanced localization techniques are used. Currently, ISIS (Ordidge et al., 1986), STEAM (Frahm et al., 1987; Merboldt et al., 1990) or PRESS (Bottomley, 1987) sequences are most frequently used as single-voxel or CSI techniques for localized MRS. Proton MRS performed with long or better, short echo times allows the quantitation of important metabolites (Frahm et al., 1989; Kreis et al., 1990; Narayana et al., 1991; Hennig et al., 1992; Ross et al., 1992; Barker et al., 1993; Christiansen et al., 1993; Kreis et al., 1993a; Michaelis et al., 1993; Danielsen and Henriksen, 1994). The automation of the measurement (shimming, water suppression, acquisition) (Webb et al., 1994) and of the data processing (phasing, fitting), have lead to a fully automated exam. Additional information is obtained by spectral editing techniques that are currently used for the identification of low concentration metabolites or overlapping resonances (Provencher, 1993).

Localized ^1H MRS includes long echo time; short echo time; STEAM; PRESS; quantitative; chemical shift imaging (CSI), metabolite imaging; 'fast' metabolite images; automated;

TABLE 2. Milestones of in vivo MRS

Twelve most prevalent uses of neurospectroscopy, 1984-2001

1. Differential diagnosis of coma: neurodiagnosis of symptomatic patients
2. Subclinical hepatic encephalopathy and pre-transplant evaluation
3. Differential diagnosis of dementia (rule out AD)
4. Therapeutic monitoring in cancer \pm radiation
5. Neonatal hypoxia
6. "Work-up" of inborn errors of metabolism
7. "Added-value" in routine MRI
8. Differential diagnosis of white matter disease especially MS, ALD and HIV
9. Prognosis in acute C.V.A. and stroke
10. Prognosis in head injury
11. Surgical planning in temporal lobe epilepsy
12. Muscle disorders

functional. ^{31}P MRS includes pulse-acquire; DRESS; ISIS; PRESS; proton decoupled ^{31}P MRS; nuclear Overhauser effect (NOE) enhanced; CSI, fast phosphocreatine metabolite imaging; magnetization transfer (flux) measurements. ^{13}C includes pulse-acquire, CSI, proton decoupled, NOE enhanced, polarization transfer, ^{13}C -labeled glucose or ^{13}C acetate (unpublished work in this laboratory) infusion flux studies. Each method has contributed to some aspect of neurochemical research or has found clinical application. All of the methods offer useful and specific information. An example would be the renewed interest in ^{31}P MRS with proton-decoupling, to identify separately the components of the "Choline" peak seen in routine ^1H MRS (see below).

The Appendix to this article offers practical information and examples of how researchers can design proton MRS experiments on typical clinical scanners.

Milestones of Neurospectroscopy

The milestones of neurospectroscopy are summarized in Table 2. MRS in

the brain began with ^{31}P spectroscopy in anesthetized rats and other small animals. Non-invasive assays of adenosine triphosphate (ATP) and phosphocreatine (PCr) (expressed as "metabolite ratios") and of intracellular pH gave exciting new insights. Direct metabolic rate determination in vivo, using ^{31}P magnetization transfer was among the first biological applications of this now widespread technique. MRS confirmed the dependence of cerebral energetics upon oxidative metabolism and glycolysis.

A practical future for MRS was demonstrated in the gerbil "stroke" model, when carotid ligation was clearly shown to produce ipsilateral changes of anaerobic metabolism: loss of PCr and ATP, increase of inorganic phosphate (P_i) and acidification of the affected hemisphere (Thulborn et al., 1981). A satisfying synthesis of some of the new neurophysiology with clinical management comes in studies of a stroke model. *Spreading depression* is the term applied to the depolarizing condition that is mimicked by high K^+ cell incubation (Bardar-Goffer et al., 1992; have explored this extensively in tissue slices), and that likely occurs with energy failure and hypoxia after stroke. Hossman (1994) and Gyngell et al. (1995) have brought diffusion weighted imaging [DWI; for a basic description, see Mori and Barker, 1999], MRS and electrophysiology together to provide new insights into growth of infarcts in rats. In short, the depolarization, which in vitro accelerates glycolysis, is detected in regions where excess lactate appears in 'bursts' within penumbra or spreading depression. The authors conclude that this physiological evidence of deterioration can be monitored by MRS, and segregated from true infarcts by diffusion weighted imaging. Removal of lactate and recovery of the neuronal marker *N*-acetyl aspartate (NAA; see below) are likely to be excellent end-points in the newly emerging clinical trials of brain salvage post stroke (Gyngell et al., 1995). It is hard now to realize that before MRS, rapid-freezing of whole animals, brain-blowing and surgical biopsy were the only effective source of knowledge of such events.

MRS in the human brain, which began with newborns, verified the

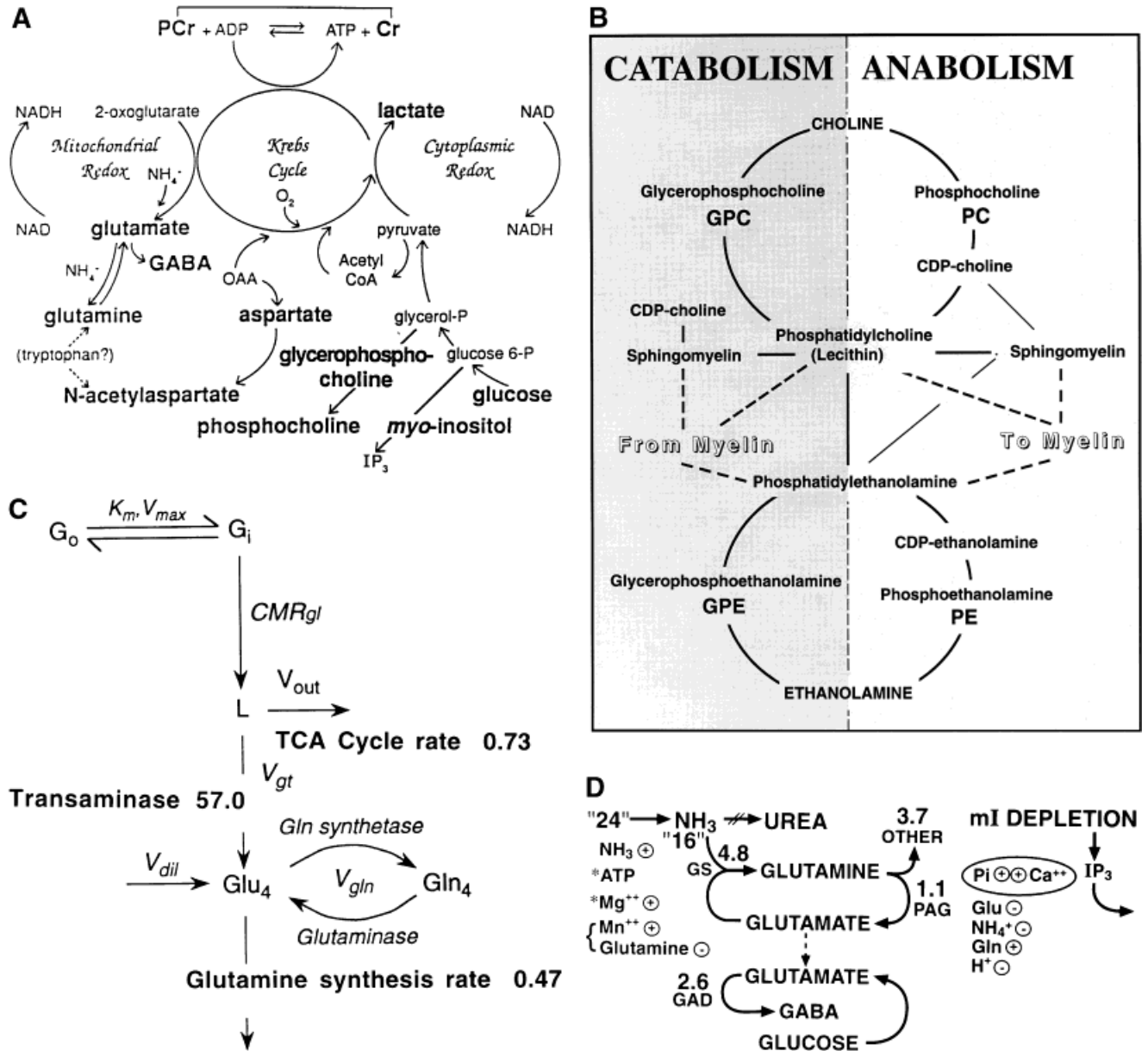


Figure 1. Neurochemical pathways: the new neurochemistry. Reactions and metabolites now readily observed *in vivo* are shown diagrammatically. **A:** Proton and phosphorus MRS. **B:** Choline and ethanolamine metabolites of "myelination" observed through proton-decoupled phosphorus MRS (figure courtesy of Prof. D. Leibfritz). **C:** Carbon fluxes detected with ^{13}C -glucose enrichment. **D:** (figure courtesy of Dr. G. Mason). Nitrogen fluxes detected with ^{15}N -ammonia enrichment (figure courtesy of Dr. K. Kanamori).

predictions of animal studies that hypoxic-ischemic disease of the brain could be monitored by the changes in high-energy phosphates, P_i and pH (Cady et al., 1983; Hope et al., 1984; Hamilton et al., 1986). The predictive value of MRS has been demonstrated in several hundred newborn infants. The outcome after severe hypoxic ischemic encephalopathy in newborn humans is determined by the intracerebral pH and P_i /ATP ratio.

Wide-bore high-field magnets permitted extension to adults and infants beyond a few weeks of age (Bottomley et al., 1983). Three areas of human neuropathology have as a result been extensively illuminated by ^{31}P MRS. Using brain tumor as a target of newly evolving localization techniques (the early studies in infants employed no localization beyond that conferred by the "surface coil"), Oberhaensli et al. (1986) began the slow process of overturning three decades of thought about brain

tumors in particular, showing their intracellular pH to be generally alkaline, not acidic. A new generation of drugs in oncology will be designed to enter alkaline intracellular environments, rather than the acidic environment measured in the interstitial fluid.

The ^{31}P MRS in adult stroke exactly mirrored the findings in hypoxic-ischemic disease of newborns, and even seems to offer predictive value through intracellular pH and P_i /ATP (Welch, 1992). This work in turn has provoked

TABLE 3. Absolute concentrations of brain metabolites in individuals of different age groups in mmol/kg brain tissue (mean \pm 1 SEM) and significance tests for differences found*

Group	n (ROIs)	GA (weeks)	pn age (weeks)	NAA	Cr	Cho	ml
<42 GA	11	38.7 \pm 0.7	3.9 \pm 1.6	4.82 \pm 0.54 ^a	6.33 \pm 0.32	2.41 \pm 0.11	10.0 \pm 1.1
42-60 GA	8	50.2 \pm 1.8	9.3 \pm 1.9	7.03 \pm 0.41	7.28 \pm 0.28	2.23 \pm 0.06	8.52 \pm 0.92
<2 pn	6	40.0 \pm 1.0	0.8 \pm 0.2	5.52 \pm 0.64	6.74 \pm 0.43	2.53 \pm 0.12	12.4 \pm 1.4
2-10 pn	7	41.9 \pm 1.5	3.8 \pm 0.9	5.89 \pm 0.21	6.56 \pm 0.44	2.16 \pm 0.09	7.69 \pm 0.62
Adult	10		1,440 \pm 68	8.89 \pm 0.17	7.49 \pm 0.12	1.32 \pm 0.07	6.56 \pm 0.43
p < 42 GA vs. adult				<0.0001	<0.0001	<0.0001	0.001
p < 42 GA vs. 42-60 GA				.0007	0.02	0.07	0.10
p 42-60 GA vs. adult				<0.0001	0.16	<0.0001	0.0003
p 42-60 2 pn vs. adult				<0.0001	0.005	<0.0001	<0.0001
p 2 pn vs. 2-10 pn				0.7	0.8	0.02	0.004
p 2-10 GA vs. adult				<0.0001	0.001	<0.0001	0.007

*GA, gestational age; pn, post-natal age; ROI, region of interest.

a large body of research in experimental models of stroke that now guides the human application of MRS.

The third area of work stimulated by the advent of ³¹P MRS was that of neurodegenerative diseases, including Alzheimer disease (Pettegrew et al., 1984). Commencing with in vitro studies of tissue extracts, two hitherto unrecognized groups of compounds, seen in the ³¹P spectrum as phosphomonoesters (PME) and phosphodiester (PDE), were empirically shown to be altered. The metabolic significance of these "peaks" was incompletely understood. Nevertheless, a promising new area of neurochemistry was opened by ³¹P MRS, and then extended to in vivo brain analysis. By providing non-invasive assays of less well-known metabolites and pathways, MRS has identified a "New Neurochemistry." A perfect example of this new knowledge emerged with the advent of water suppressed ¹H MRS of the brain in vivo.

NAA, a neuronal marker (Tallan, 1957), was re-discovered in 1983 (Prichard et al., 1983). Of the many expected and new resonances now identified in human neuro-MRS, none has yielded more diagnostic information than NAA. Its identity, concentration and distribution are now well estab-

lished. Early experiments in animals showed loss of NAA in stroke. Very large numbers of studies in man show NAA absent, or reduced in brain tumor (glioma, see Figure 2), ischemia, degenerative disease, inborn errors and trauma, so that to a first approximation, the histochemical identification of NAA (and *N*-acetylaspartyl glutamate [NAAG]) with neurons and axons, and its absence from mature glial cells, is confirmed. The use of ¹H MRS as an assay of neuronal "number" seems well justified.

The first generation of human MRS studies were performed without image-guidance. Although MRI is not essential to our understanding of neurochemistry, the combined use of these two powerful tools permitted the direct demonstration that there is often a dissociation in space, between anatomically obvious events in the brain and biochemical changes. Metabolite imaging has confirmed this important principle in stroke, tumors, multiple sclerosis and degenerative diseases.

A simplified method of localization permitted the routine use of MRS to assay neurochemistry in a single place, albeit rather large, in the cerebral cortex, cerebellum or mid-brain. This method, now generally known as "single-voxel MRS" is largely respon-

sible for showing that biochemical disorders commonly underlie neurological disease (Prichard et al., 1983; Hanstock et al., 1988; Frahm et al., 1988, 1989, 1990; Kreis et al., 1990; Michaelis et al., 1991; Ross et al., 1992; Stockler et al., 1996). MRS is therefore well poised for "early" diagnosis. Reversible biochemical changes accompany several physiological events, and provide a biochemical basis for functional imaging (fMRI) (Merboldt et al., 1992; see also Beckmann et al., 2001; Zeineh et al., 2001). The inborn errors of metabolism and hereditary diseases, and several of the major neurological scourges of our time, reveal functional biochemical disturbance. Neonatal hypoxia, cerebral palsy, neuro-AIDS, dementias, stroke, epilepsies, neuro-infections and many encephalopathies are now seen to include a biochemical component.

Automation and quantitation are the final ingredients required to make MRS an indispensable tool in human neuroscience. Automation permits universal access, including urgent MRS in acute, reversible neurological diseases, and large scale clinical trials. Quantitation, a long-overlooked area, gives the precision of measurement that will be required to conclusively

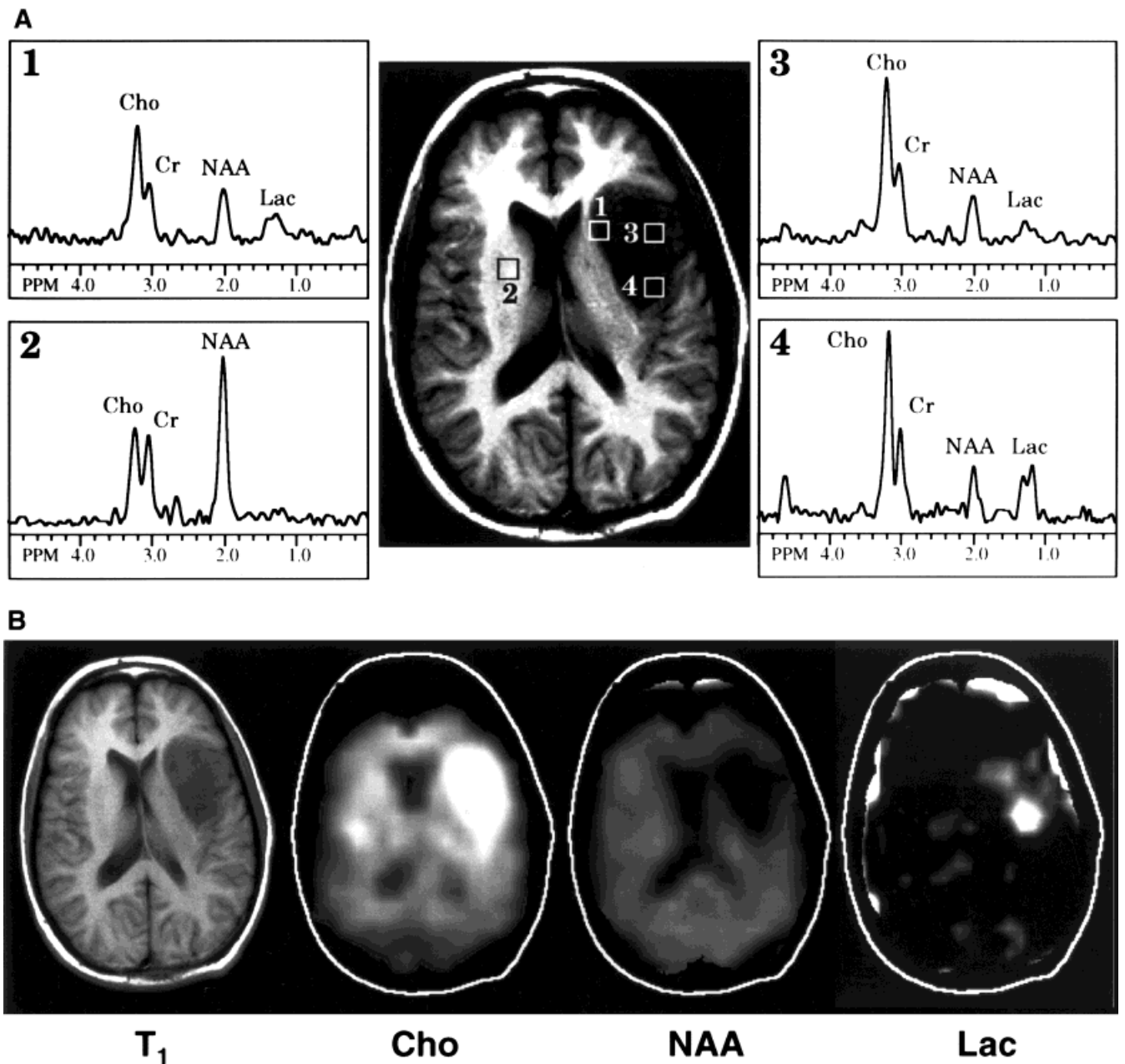


Figure 2. CSI: Heterogeneous metabolism of brain tumor. **A:** Local concentrations of each of the four principal metabolites to be recorded during a single MRS-examination. **B:** Results are displayed as metabolite-images (courtesy of Dr. P.B. Barker).

demonstrate incremental metabolic responses to intervention or therapy.

CHEMICAL COMPOSITION OF THE BRAIN

Although obviously an oversimplification, in MRS-terms brain may be biochemically defined as water plus dry-matter.

Brain-Water

The water, as in other tissues, is divided into intracellular and extracellu-

lar (about 85% and 15% respectively). Intracellular water, which is further divided into cytoplasmic and mitochondrial compartments, about 75% and 25% respectively, contains all of the important neurochemicals (e.g., Figures 3–6). These are either unique to intracellular water, such as lipids, proteins, amino acids, neurotransmitters and low-molecular weight substances, or at least have a very different concentration from the extracellular and cerebrospinal fluid (CSF) compartments. Glucose is an excep-

tion, being found in proportions 5:3:1 in blood, CSF and brain-water respectively. Amino acids are generally distributed 20:1, brain water:CSF or blood. Brain water and extracellular fluid (ECF) are distinct from the large CSF compartment, the volume of which depends greatly upon the location selected, and from the intravascular blood, which comprises up to 6% of brain water. MRS-assays of brain water represent the sum of intracellular fluid (ICF) and ECF (Ernst et al., 1993a).

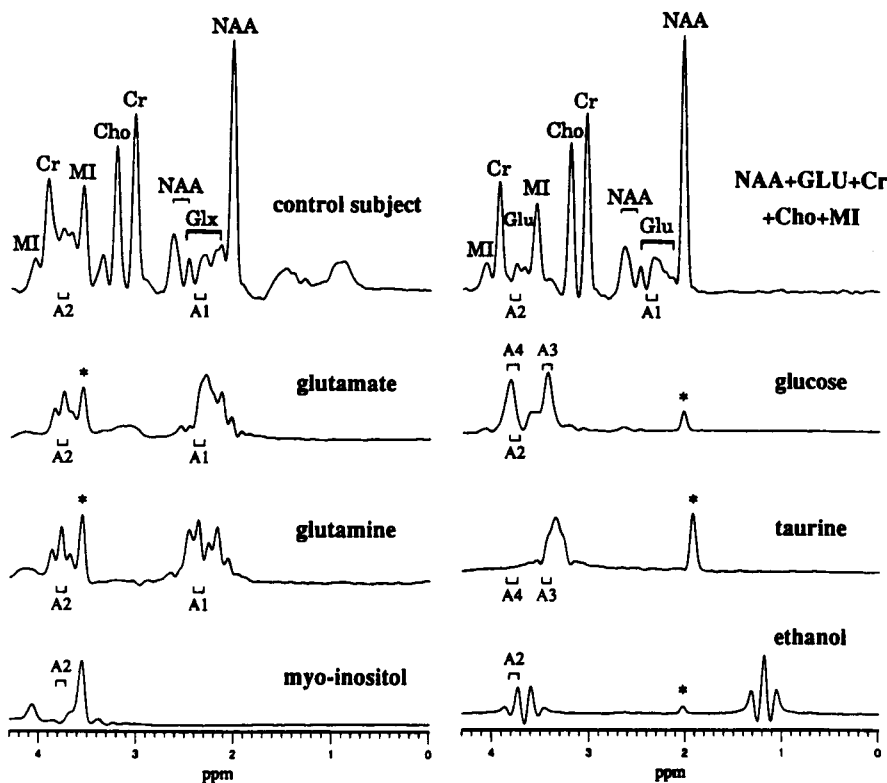


Figure 3. Localized *in vivo* and *in vitro* ^1H MR spectra acquired with a stimulated echo sequence at 1.5 T. At the top left is a normal brain spectrum (the sum of results from 10 age-matched control subjects). At the top right is a reference spectrum from an aqueous solution composed of 36.7 mmol/l of *N*-acetylaspartate (NAA), 25.0 mmol/l of Cr, 6.3 mmol/l of choline chloride, 30.0 mmol/l of glucose (Glu), and 22.5 mmol/l of ml (adjusted to a pH of 7.15 in a phosphate buffer). The remaining spectra were recorded from solutions of individual biochemicals. To simulate *in vivo* conditions, all spectra were subjected to a line-shape transformation yielding gaussian peaks of approximately 4 Hz line width. The integration ranges used to detect changes in the cerebral levels of Glx (Glu or glutamine (Gln)) (A1 + A2) and Glu (A3 + A4) are indicated. The peaks labeled * originated from glycine, NAA, or acetate, which were added to the various solutions as chemical shift references (the methyl peak of NAA was set to 2.02 ppm). All spectra were scaled individually and cannot be used for direct quantitation (modified from Kreis et al., 1992, with permission of the publisher).

Brain Dry-Matter

Seen through the MR image and the MRS assays of water, the 20% or so of brain that really “matters” is largely invisible! Hence the terms “missing” or “invisible” are found occasionally in the MRS literature. Covered by these terms are all macromolecules (DNA, RNA, most proteins and phospholipids), as well as cell membranes, organelles, including the dry-matter of the mitochondria, the cristae, and myelin. The term is probably equivalent to the biochemist’s “dry-weight” and can be used as a more constant unit by which to determine the concentration of key neurochemicals. This is particularly relevant in pathologies in which brain water (or wet-weight/dry weight) may alter, such as metabolic disorders, edema, tumors,

inflammation, stroke or infarction. Metabolite concentrations may therefore more accurately be compared as mmol/g dry weight than by the more usual mmol/g wet weight, or per ml of brain water.

Myelin and Myelination

For the most-part myelin is inaccessible to *in vivo* MRS (because of the manner in which myelin water contributes to the MR signal, the contrast between white and gray matter is striking in MRI). The composition of myelin is nevertheless of some interest to the *in vivo* spectroscopist because of the changes that may occur in demyelinating and many other diseases. Although major components like phosphatidyl choline, phosphati-

dyl-ethanolamine, -serine and -inositol are probably entirely immobile and NMR-invisible, their putative breakdown products, such as phosphoryl choline, glycerophosphoryl choline, choline, and *myo*-inositol, are a normal feature of the ^{31}P or ^1H brain spectrum. These molecules will be frequently encountered in discussions of clinical spectroscopy, even though their precise relationship to myelin is far from clear. This is nowhere more important than in the detection of developmental changes in the brain, which are accompanied by dramatic changes in the MR spectrum (Bluml et al., 1998).

Edema

This all-important concept in neurophysiology and in clinical diagnosis by DWI and MRI, has not yet been clearly defined in MRS assays of brain water. One possibility is that edema, as seen in MRI, represents less than

The predictive value of MRS has been demonstrated in several hundred newborn infants.

1% of total brain water, and falls within the limits of error of present methods of NMR water assay. These methods rely heavily upon differences in T_2 between water in various states. Although it is T_2 that distinguishes edema in MRI, the differences are either too small or too local to be measured directly with MRS.

Metabolism

Amino acids, carbohydrates, fatty acids and lipids, including triglycerides, form a complex network of biosynthetic and degradative pathways. The network is maintained by the thermodynamic equilibrium of hundreds of identified enzymes, and relative rates of flux through the various pathways are equally closely controlled. Hence, the concentrations of all but a few key molecules (messengers and neurotransmitters) are kept remarkably constant (e.g., Table 3, Figure 6, 7 and

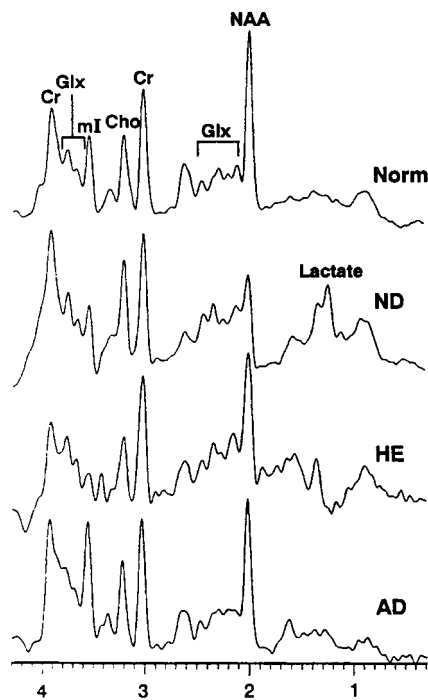


Figure 4. ^1H MR spectra of gray matter acquired with PROBE. ^1H MRS of gray matter acquired with PROBE. The top spectrum is taken from a healthy volunteer. Spectra from global hypoxia due to near-drowning (ND) (spectrum 2), hepatic encephalopathy (HE), and probable Alzheimer disease (AD) are shown. All spectra were acquired on a 1.5 T scanner using stimulated-echo acquisition mode (STEAM) and short echo time TE = 30 ms; repetition time TR = 1.5 s.

8). It is for this reason that a thoroughly reproducible brain “spectrum” can be obtained with MRS. Conversely, predictable and reversible changes, such as increased lactate and glutamate, reduced ATP and increased ADP, due to altered redox state of the pyridine nucleotide coenzymes of electron transport do occur. This makes MRS the tool for short-term studies on the brain. A comprehensive list of brain metabolites studied using MRS is given in Table 4.

Compartmentation

Mitochondrial energetics, the enzymes of which are controlled by non-Mendelian genetics, consists of the electron-transport chain and of oxidative phosphorylation that provides virtually all of the high-energy phosphate bonds to maintain ion pumps, neurotransmission, cell volume and active transport of nutrients. ATP, the essential “currency” of this process, is buffered in brain by another high-energy

system, that of creatine-kinase, creatine (Cr), and phosphocreatine (PCr). These molecules are readily observed in MR spectra. Cytoplasmic enzymes control aerobic glycolysis and the formation of lactate, which supplements ATP synthesis. Glycolysis is massively activated by the Pasteur effect under hypoxic conditions that obviously limit mitochondrial energy production. Lactate and glutamate are both formed in excess when the mitochondrial redox state changes. It is possible that a similar activation of glycolysis accompanies “functional” changes (as in fMRI; see Zeineh et al., 2001) and electrical activation (in seizures). It should be noted, however, that mitochondrial metabolite pools are to a variable extent NMR-invisible and may not contribute to the final brain spectrum.

Fuels of Oxidative Phosphorylation

Glucose dominates the fuel supply for brain, and its supply via blood flow is strenuously protected. Vascular occlusion, because it brings with it glucose deprivation, oxygen lack, and CO_2 and H^+ accumulation, results in rather different neurochemical insults from that of pure hypoxia, such as is seen in respiratory failure or near-drowning. Thus, hypoxia and ischemia are different to the spectroscopist whereas the terms might not need to be distinguished for the purposes of MRI.

Under severe conditions of starvation, when glucose is not available, fatty acids (including acetate) and ketone bodies can sustain cerebral energy metabolism, and this may be the normal state of affairs for the milk-fed newborn. Unlike other tissues, the brain does not apparently require insulin to utilize glucose, so in diabetics the marked alterations in cerebral metabolism (and in the MR spectrum) are secondary to the systemic metabolic disorder. Finally, it is now clear that ‘two pools’ of cerebral glutamate metabolism involved in neurotransmission represent astrocytes (small-pool) for which acetate is the preferred fuel, and neurones (large-pool) for which glucose metabolism predominates. An exciting opportunity therefore exists to interrogate these two cell populations independently,

within the living brain, simply by altering the fuel supplied in a ^{13}C MRS study for example (see below).

Brain Metabolism: A Summary

Figure 1A–D depicts some of the neurochemical pathways that have become more relevant since the advent of neuro-MRS. The energetic interconversion of ATP, PCr and P_i , together with intracellular pH is readily monitored by ^{31}P MRS. The major peaks of the ^1H MR spectrum, *N*-acetylaspartate (NAA), total creatine (creatine plus phosphocreatine; Cr), total choline (as reflection of phosphoryl choline and glycerophosphoryl choline; Cho), *myo*-inositol (mI), and glutamate plus glutamine (Glx), were only infrequently encountered in neurochemical discussions of

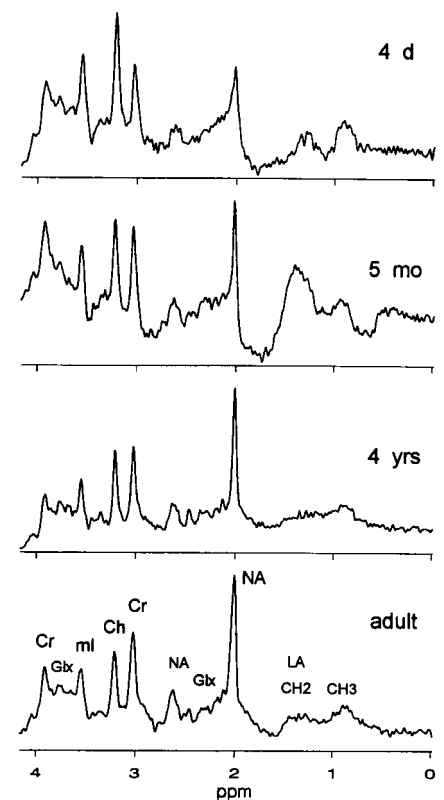


Figure 5. Typical cerebral MR spectra for subjects of different age. Typical cerebral proton MR spectra from subjects of different ages. Relative amplitude of the main peaks in STEAM spectra vary drastically with age. Spectra were obtained from a periventricular area in the parietal cortex. Acquisition parameters: echo time TE = 30 ms, repetition time TR = 1.5 s, 144–256 averages, voxel sizes 8–10 cm^3 for children, 12–16 cm^3 for adults (modified from Kreis et al., 1993b, with permission of the publisher).

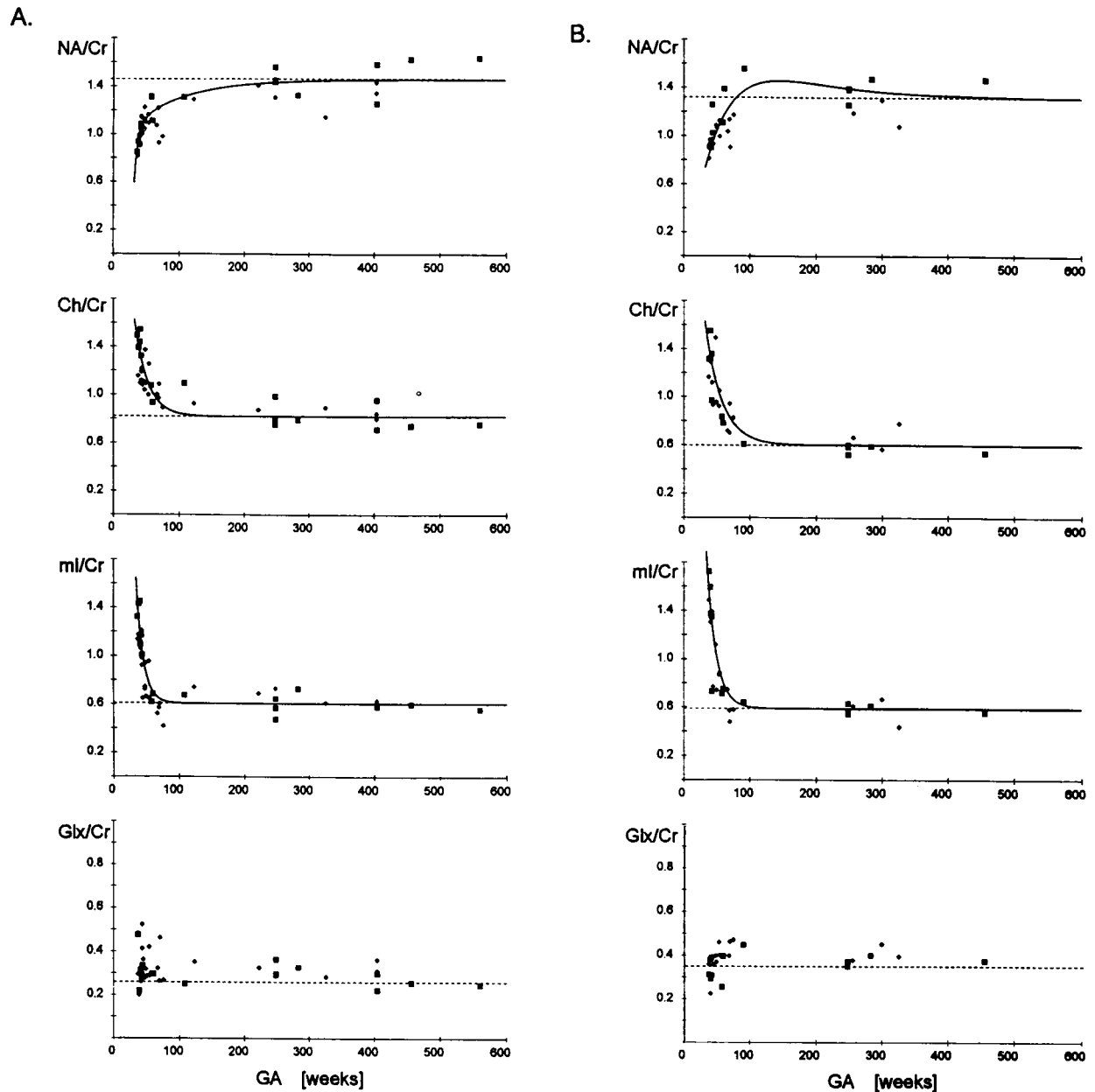


Figure 6. Time courses of metabolite peak amplitude ratios vs. gestational age of the subject. Time courses of metabolite peak amplitude ratios vs. gestational age of the subject. **A,B:** Normative curves for the parietal (mostly white matter) and occipital (predominantly gray matter) locations, respectively. The ratios were calculated as detailed in (Kreis et al., 1991). Cho/Cr and ml/Cr were fitted to a mono-exponential, whereas NAA/Cr was fitted to a bi-exponential model function. No developmental curve was calculated for Glx/Cr data, because no clear trend was visible. The curves are well defined for the 1st year of life, where the most dramatic changes take place. Features in the later stages of development are less accurately described by the present data. The normative curves are specific for the acquisition parameters used. Open symbols represent data from parietal cortex, and filled symbols data from occipital cortex.

physiology or disease, before the advent of MRS. They now join glucose uptake and oxygen consumption as the most easily measured neurochemical events, and must become increasingly important in neurological discussion. The interconversion of phosphatidylethanolamine and phosphatidylcholine (by transmethylation) explains the close links between mye-

lin products now quantifiable through proton-decoupled ^{31}P MRS (Fig. 1B).

Because of the concentration limit (of protons) at about 0.5–1.0 mM for NMR-detection, virtually all true neurotransmitters, including acetylcholine, norepinephrine, dopamine, serotonin (the exceptions are glutamate, glutamine and GABA) are currently beyond detection by conventional

neuro-MRS. Similarly, the second messenger inositol-polyphosphates and cyclic AMP are not detected. This leaves important gaps in the New Neurochemistry.

Another evident shortcoming of NMR is the inaccessibility of most macromolecules because of their limited mobility. Accordingly, phospholipids, myelin, proteins, nucleosides

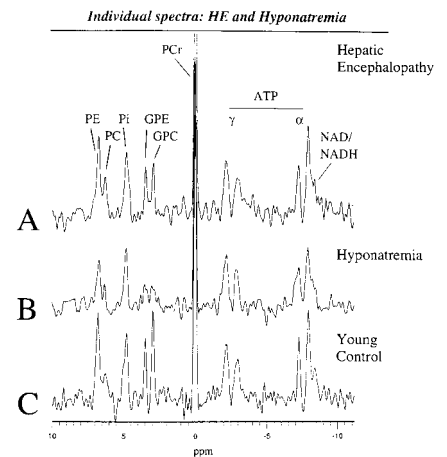
TABLE 4. Cerebral metabolites measured in vivo by MRS

Name of Metabolite	Technique	Precision
Acetoacetate	^1H	± 0.5 mM
Acetone	^1H	± 0.3 mM
Adenosine-triphosphate (ATP)	^{31}P	± 0.2 mM
Aspartate	^1H	± 2 mM
Atrophy index	^1H	$\pm 1\%$
Beta-hydroxybutyrate	^1H	± 0.5 mM
Brain dry-matter	^1H	$\pm 2\%$
Choline	^1H	± 0.1 mM
Creatine	^1H	± 1 mM
CSF-peak aqueduct flow	^1H -Cine	± 3 ml/min
CSF-volume	^1H	$\pm 1\%$
Ethanol	^1H	± 1 mM
Fluoxetine	^{19}F	± 1 microg/ml
(Tri)fluoperazine	^{19}F	± 1 microg/ml
GABA	^1H	± 1 mM
Glucose	^1H , ^{13}C	± 0.5 mM (?)
Glucose transport rate (T_1/T_2)	enr ^{13}C	± 1.5 min
Glutamate	^{13}C	± 2 mM
Glutamine	^1H	± 1 mM
Glycerol	^{13}C	± 5 mM
Glycerophosphorylcholine	{ ^1H }- ^{31}P	± 0.2 mM
Glycerophosphoethanolamine	{ ^1H }- ^{31}P	± 0.2 mM
Glycine	^1H	± 1 mM
Glycolysis rate	en ^{13}C	± 0.37 /min/g
Guanosine-phosphate	^{31}P	± 1 mM
Hydrogen-ion (pH)	^{31}P	± 0.02 pH units
Inorganic phosphate	^{31}P	± 0.2 mM
Inositol-1-phosphate	{ ^1H }- ^{31}P	yes or no
Isoleucine	^1H	± 1 mM
Lactate	^1H	± 0.5 mM
Leucine	^1H	± 1 mM
Lipid	^1H ; ^{13}C	± 1 mM
Lithium	^7Li	± 0.1 mM
Macromolecules	^1H ; ^{13}C	± 0.1 mM
Magnesium (Mg^{++})	^{31}P	± 200 mM
Mannitol	^1H	± 2 mM
Myoinositol	^1H ; ^{13}C	± 1 mM
NAA	^1H	± 0.7 mM
NAAG	^1H	± 0.3 mM
Oxydized hemoglobin	fMRI (^1H)	$\pm 0.2\%$
Phenyl-alanine	^1H	± 2 mM
Phospho-choline	dc ^{31}P	± 0.2 mM
Phosphocreatine	^{31}P	± 0.2 mM
Phosphodiester	^{31}P	± 2 mM
Phosphoethanolamine	dc ^{31}P	± 0.1 mM
Phospholipid (membrane)	dc ^{31}P	$\pm 30\%$
Phosphomonoesters	^{31}P	± 2 mM
Propane-diol	^1H	± 1 mM
Pyridine nucleolide(s) (NAD, NADP)	dc ^{31}P	± 1 mM
Scylloinositol	^1H	± 0.2 mM
Sodium	^{23}Na	\pm
Taurine (see also sl)	^1H	± 1 mM
TCA-cycle rate	enr ^{13}C	± 0.1 $\mu\text{mol}/\text{min}/\text{g}$
Transaminase rate	enr ^{13}C	± 10 $\mu\text{mol}/\text{min}/\text{g}$
Triglyceride	^{13}C	± 5 mM
Valine	^1H	± 1 mM
Water content	^1H	$\pm 3\%$

enr, enriched; dc, decoupled; ^1H -Cine, cine-MRI. Current techniques of MRS on "clinical" MR scanners permit quantifiable assays of each of these metabolites, fluxes or neurochemical events in examination times tolerated by the average volunteer or patient. Not all tests are available on every commercial scanner.

Box 2. Representative $\{^1\text{H}\}$ - ^{31}P MRS Spectra of Diseased Brain in Adults: Hepatic Encephalopathy, A Disorder of Cerebral Osmoregulation?

Accumulation of ammonia in the blood causes a series of very specific changes in ^1H MRS of hepatic encephalopathy (HE). Expected and readily explained by the conversion of ammonia and glutamate into glutamine is an increase of cerebral glutamine. Changes of other metabolites such as a depletion of *myo*-inositol and a reduction in choline, however, are not completely understood. Proton decoupled ^{31}P MRS can significantly improve our understanding of the pathophysiology of HE by measuring the Cho constituents separately, quantifying brain phosphoethanolamines, and high energy metabolites. **A:** In this HE patient a reduction in GPE and the recognized osmolyte GPC can readily be detected whereas PC is unchanged. When groups of patients and controls were compared statistically significant reduction of PE, P_i , and ATP were observed. These findings support the hypothesis of a disturbed osmoregulation. The suggestion that HE is accompanied by cerebral energy failure is supported by the findings of $1\text{-}^{13}\text{C}$ glucose MRS, despite the absence of the classical pattern of reduced PCr and elevated P_i . **B:** Hyponatremia is recognized to cause a disorder of cerebral osmoregulation. The spectrum from a patient with hyponatremia of unknown cause (not HE) seems to have a similar pattern as in HE but with the abnormalities even more pronounced. **C:** Typical spectrum from a young control for comparison (figure modified from Bluml et al., 1998, with permission of the publisher).



and nucleotides, as well as RNA and DNA are effectively “invisible” to this family of methods. Exceptions may be glycogen, a macromolecule in heart, skeletal muscle and liver, which is readily detectable in ^{13}C spectra, and the broad signals from phospholipids in the ^{31}P spectrum and from low molecular weight proteins in ^1H spectra in the brain.

Flux measurements using enriched stable-isotopes of ^{13}C (Fig. 1C) or ^{15}N (Fig. 1D) extend the range of neurochemical events accessible to in vivo MRS. More than 50 metabolites can now readily be determined by combination of these techniques (Table 4).

Technical Requirements and Methods

Many years of experience with clinical MRI have resulted in a widespread and comfortable understanding of the MR process. The patient (or subject) must be able to lie on a bed, which enters a confined space where electromagnetic fields are repeatedly switched on and off. The subject must tolerate the accompaniment of considerable noise. After an interval of one to several minutes, all of the radio-signals generated by resonating protons are mathematically mapped to produce an image. The anatomical display in cross-section is now the norm for all who work in the brain.

MRS is produced in the same way, with three *additional steps*. Using the image just obtained, a volume of interest (VOI; voxel) is selected for MRS and the field within is further refined in a process called *shimming* (shim: old English, a wedge or plough-share). Then, for ^1H MRS (but not for MRS of other nuclei), the protons of H_2O within the VOI are rendered silent by suppressing their particular frequency band (termed *water suppression*). Finally, using the same constellation of switched magnetic fields already familiar from MRI, a frequency profile or spectrum is acquired. Intensity at any given frequency is proportional to concentrations of protons. Frequency is a measure of chemical structure; thus the spectrum is a typical output of metabolite composition of the sample.

In MRI, where localization is “everything,” only a single peak (^1H of water) is mapped. In MRS, localization must retain chemical shift information for the acquisition of metabolite profiles (Ordidge et al., 1985). Single-volume (or voxel) MRS uses methods that allow to measure MR signals originating from one region of interest and ensures that unwanted MR signals outside this area are excluded. Alternative strategies exist. *Selective excitation* is analogous to MRI, in which a single metabolite frequency is excited and an image is reconstructed. Mapping of cerebral

phosphocreatine (PCr) has employed this technique (Ernst et al., 1993b). *Chemical-shift-imaging* (CSI) acquires simultaneously multiple spectra from slices or volumes of the brain (Fig. 2A) and metabolite specific images are readily formed from the resulting peak-intensities (Fig. 2B). Although theoretically the most time-efficient method of in vivo neurochemical analysis, in practice CSI brings with it many unwanted features such as loss of metabolic information, unexpected quantitative variability across the “slice,” and inconveniently bulky data sets. At this point, *single-voxel MRS* dominates the field of in vivo brain MRS.

For single-voxel MRS, manufacturers provide one or more of the following capabilities:

- STEAM (stimulated echo acquisition mode),
- PRESS (point resolved spectroscopy), and
- ISIS (image selected in vivo spectroscopy).

Technical details, selection criteria and the necessary physics are extensively discussed in Young (2000).

Hardware and Equipment

Relatively few research organizations have the capability to design and build human MR scanners, and stringent National and International regulations control their use. The MR equip-

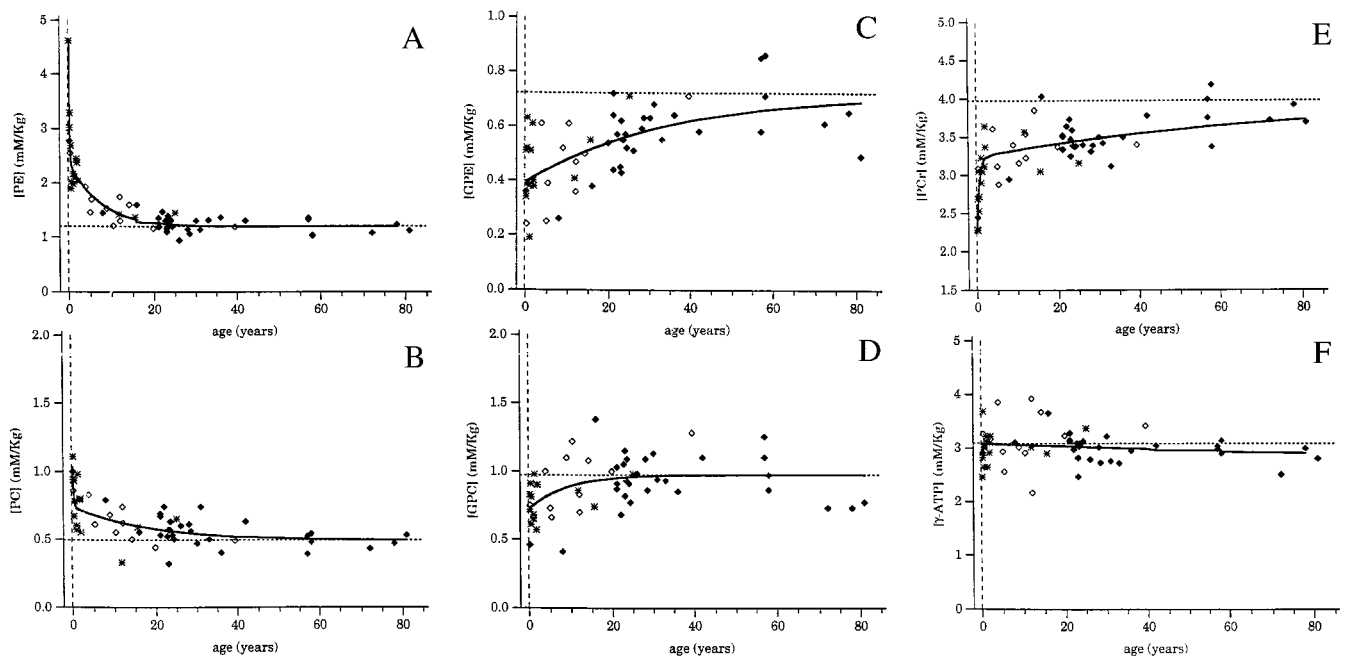


Figure 7. Age related changes of absolute concentrations of the membrane metabolites PE, PC, GPE, GPC and high energy metabolites PCr and ATP. (PE) (A) and to a lesser extent (PC) (B) decrease with age. Adult levels are reached at age >12 years. (GPE) (C) and (GPC) (D) increase only slightly with age. (PCr) (E) increases whereas (ATP) (F) shows a mild decrease with age. Age was corrected for gestational age where applicable.

ment is large, heavy and expensive to site, in magnetically shielded rooms, usually remote from other equipment. Whole-body, or slightly smaller “head-only” units are available. Clinical equipment is rarely more than 1.5 or 2.0 Tesla, but even in the Clinic, 3 Tesla, 4 Tesla or 4.7 Tesla are becoming commonplace. Seven Tesla, 8 Tesla and 9.4 Tesla are in an exploratory stage but likely to become equally indispensable tools in the Neuroscience Research Institute of the future.

A Word About Safety

Three different magnetic fields are applied in MRS:

- static magnetic field B_0 ;
- gradient fields for localization purposes, and
- rf fields to excite the magnetization.

These fields are remarkably safe, with no known biological hazards. Fast switching gradients have been considered as associated with risk, but never more than vaguely identified. Although there exist “exotic” techniques such as echo planar spectroscopic imaging (EPSI), the vast majority of MRS techniques switch gradients a magnitude slower than

routinely applied in MR imaging. Prolonged irradiation of RF is identified as hazardous, to the extent that energy is “deposited” in the human head. A sensible government limit (SAR) has provided binding guidelines for nearly 20 years. Provided instruments are correctly calibrated and fitted with necessary power-monitor and automatic trip, no harm can come to subjects, voluntary or patients, during MRS studies. Isolated reports of burns from faulty electrical equipment, home-built RF coils, guide wires and electrodes are rarely serious but are a sure sign of sloppy science and cannot be tolerated in a first class Neuroscience Institute.

A different class of safety deals with magnetic objects. Scissors, knives, scalpels, etc., brought into the vicinity of the magnetic field become fast projectiles and can cause serious injuries. Also implanted metallic objects can cause serious harm to a patient as a consequence of electrical interaction, torque, or heating before or during an examination. Therefore, physical safety around MR equipment is a matter of great concern. Every unit should have a Safety Officer, a clear code of conduct and probably metal detectors at all public entrances. Lax security

results inevitably in “accidents” that could have been avoided with conscientious management. Safety lies in excellence of the design of the MR-Suite and military-style discipline.

RF Coils and Gradients

MRI and ^1H MRS of brain is usually undertaken with a standard volume head coil constructed like a helmet to fit over the entire head, and is provided by the manufacturer. For specialized purposes, and because in general they furnish much needed extra signal, surface coils or an assembly of surface coils (termed *phased-array*) are used. Volume coils are more flexible and have a special advantage when quantitation of cerebral metabolites is the goal.

Because a ^1H head coil is standard equipment on all scanners, proton MRS is in principle available on all clinical scanners and by far the most widely used MRS technique. RF coils are frequency-specific, however, so that MRS studies with other nuclei than proton demand a different (and costly) head coil. Often these coils are not provided directly by the manufacturer but need to be purchased from smaller suppliers. For proton-de-

coupled MRS, which has increased sensitivity and other advantages in MRS of nuclei other than proton (X-nucleus), combined RF coils, H + X, are the norm. Again, these types of coils are often not among the options offered by the manufacturer of the system but need to be purchased separately.

The rapid technical progress in gradient coils in recent years is mainly driven by MRI applications. In particular functional MRI and diffusion weighted MRI, utilizing echo planar imaging (EPI), requires fast switching gradients with fast rise times. Although in general MRS also benefits from more powerful gradient systems, sometimes larger eddy currents from speed and power optimized gradient coils may affect spectral quality adversely on newer systems.

Hetero-Nuclear Detection and ^1H Decoupling

Even if RF coils tuned to nuclei other than ^1H are available, not all MRI scanners can progress beyond ^1H detection. Broadband amplifiers are essential if anything other than ^1H MRS is to be undertaken. Similarly, RF receivers tuned to the resonance frequency of the nucleus to be observed must be provided along with several other hardware features that are sometimes difficult to retrofit.

Along with the capability to perform heteronuclear (other than ^1H) MRS comes the need to enhance sensitivity and specificity of chemical analyses by proton-decoupling. This involves simultaneous excitation at a different frequency, and accordingly requires a second RF channel and amplifier.

Examples of spectra that illustrate ^1H MRS quantitation, signal advantage from a surface coil compared with a volume coil, broadband-heteronuclear MRS and finally, the effects of proton-decoupling, all from the same clinical MR scanner retrofitted with the above mentioned components, are shown at the end of this chapter.

Pulse Sequences: Localization Methods

A necessary step in vivo is the segregation of extra-cerebral from intra-cerebral metabolites and of one intra-

cerebral location from another. Localization sequences select cubes, rhomboid shapes, "slices" or multiple boxes, none of which confirm to recognizable structures of the human brain. The choice of the technique is often pre-ordained by the manufacturer and is less important than the need for absolute consistency within any research program. Although marked differences in spectral appearance result, data is interchangeable between two different sequences, with some loss of precision.

RESULTS

Neurospectroscopy

Proton MRS is by far the most widely used spectroscopy technique in the brain. This is due to the fact that standard MRI hardware components are used, making ^1H MRS available, that the concentrations of protons are relatively high in the brain, and that the MR sensitivity to protons is higher than the sensitivity to other nuclei.

How to "Read" a Proton Spectrum

The proton spectrum of the normal human brain is most readily understood by referring to Figure 3. Each metabolite has a "signature" (Ross et al., 1992), which when added to the other major metabolites results in a complex spectrum of overlapping peaks. For all practical purposes, at the moment, due to ease and universal access, proton spectroscopy is synonymous with neurospectroscopy. Although such spectra are familiar to all, it is crucial to adopt a rigorous approach to acquiring and interpreting spectra.

Figure 4 is composed of 4 spectra from "gray matter" acquired by an automated procedure (PROBE™ = PROton Brain Exam), using a 1.5 T scanner, STEAM and short echo time (TE = 30 ms). The equivalent spectra acquired at long echo (TE = 135 or 270 ms) would look substantially different, but could be similarly interpreted by referring to a "normal" spectrum acquired under identical conditions.

The top spectrum (Fig. 4, "Norm") is taken from a healthy volunteer. Reading from right to left there are

two broad resonances that are believed to be due to intrinsic cerebral proteins or lipids. The first and tallest sharp peak, resonating at 2.0 ppm is assigned to the neuronal marker *N*-acetylaspartate (NAA). The next cluster of small peaks consists of the coupled resonances of *b*- and *g*-glutamine plus glutamate (Glx). The tallest peak of this cluster at approximately 2.6 ppm is actually NAA that has three

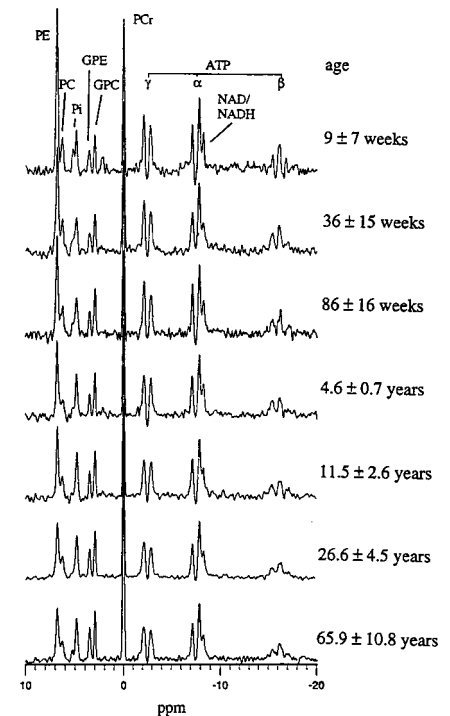


Figure 8. Normal age related changes in the spectral appearance of $\{^1\text{H}\}-^{31}\text{P}$ MRS. Shown are averaged spectra from control subjects, each calculated from a group of subjects within the age range as indicated in the figure. Most apparent is the striking reduction of PE, being the most prominent peak in a newborn, within the first weeks of life. This is contrasted by only a small reduction of the second phosphomonoester PC. Inorganic phosphate P_i peaks are observed at 4.8 and 5.1 ppm, representing an intercellular compartment and an extracellular or CSF compartment. The two peaks are separated due to the different pH intra- and extracellular, 7.0 vs. 7.2. The peak originating from extracellular P_i can be readily observed in the baby spectra because of the increased ventricles in hydrocephalus. GPE and GPC show a slight, generally increasing trend with age. A resonance at 2.2 ppm consistent with glycerophosphoryl serine or phosphoenolpyruvate was observed only in the neonate spectrum (age 9 ± 7 weeks). PCr increases with age whereas ATP slightly decreases. All spectra were processed and scaled identically to allow direct comparison (modified from Bluml et al., 1999, with permission of the publisher).

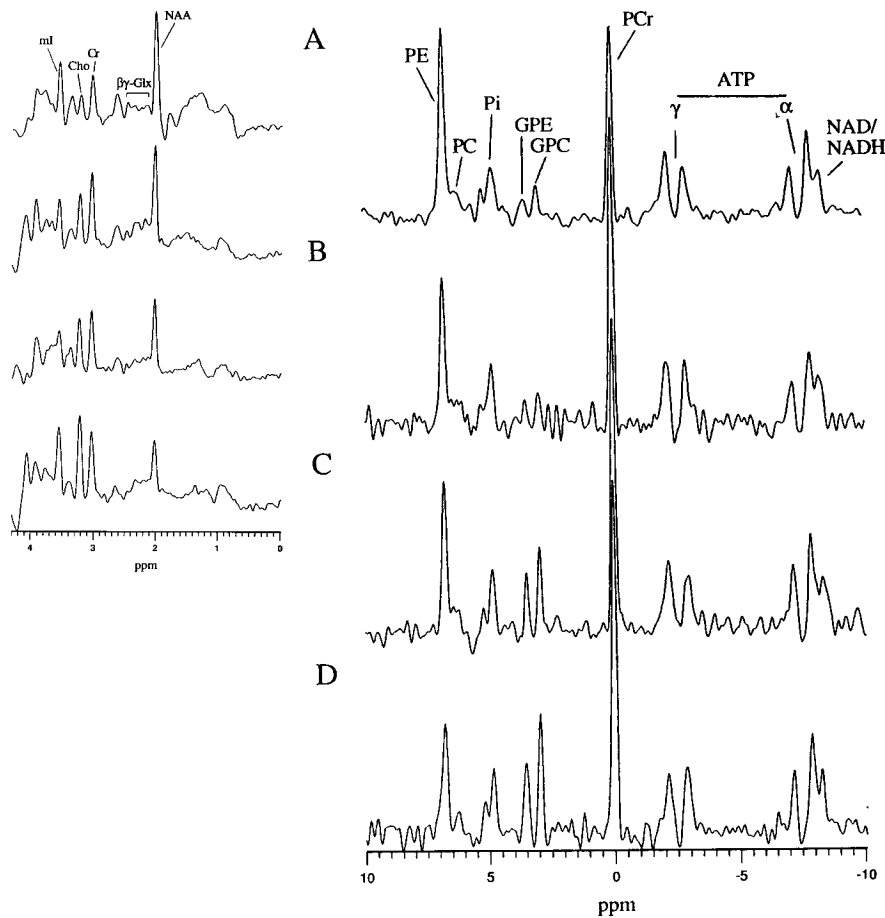


Figure 9. Representative $\{^1\text{H}\}$ - ^{31}P and ^1H MR spectra of diseased brain in babies and children. **A:** Canavan disease (aspartoacylase deficiency) presents in proton MRS with highly elevated NAA, elevated ml and reduced total Cr and Cho. Additional information about the pathophysiology of this rare inborn error is obtained by $\{^1\text{H}\}$ - ^{31}P MRS, the membrane metabolites PC, GPE, and GPC as well as the high energy metabolites PCr and ATP appearing to be reduced (see Fig. 18B for sequential proton MRS for treatment monitoring in this patient). **B:** This patient initially diagnosed with and treated for hydrocephalus did poorly clinically and showed abnormal myelination in follow-up exams. GPC was found to be reduced whereas PCr appears to be elevated. **C:** A patient with amino acid inborn error disease (glutaric aciduria II) showed elevated GPE, GPC, and PCr. **D:** In consolidated late hypoxic injury, increased GPE, GPC, and PCr may reflect a partial volume effect of increased glial cells density. In all patients, separately acquired proton MRS is consistent with $\{^1\text{H}\}$ - ^{31}P MRS findings insofar as total Cr (= free Cr + PCr) and total Cho (GPC + PC + minor contributions from other metabolites) parallels changes in PCr or GPC and PC (right panel). Inset (left panel) are the corresponding ^1H MRS for patients A-D (from above).

peaks, one of which overlaps the glutamine resonance. The second tallest resonance (at ~ 3.0 ppm) is creatine plus phosphocreatine (Cr), and adjacent to this is another prominent but smaller peak, assigned to "choline" (Cho). A small peak to the left of Cho is that of *scyllo*-inositol (sI). A prominent peak at 3.6 ppm is assigned to *myo*-inositol (mI). To the left of mI, two small peaks of the α -Glx triplet are clearly seen, and to the left is the second Cr peak. Variations in the degree of water suppression affect the peak intensities of metabolites closest to the water frequency at 4.7 ppm; i.e.,

the second Cr peak and its immediate neighbors. This effect of water suppression, however, has no influence on the diagnostic value of spectra. The three major resonances (NAA, Cr and mI) provide a steep angle up from left to right in normal spectra acquired at short TE.

In the near-drowning spectrum (Fig. 4, spectrum 2, "ND"), a lipid peak and overlying lactate doublet (at 1.3 ppm) replace the normally nearly 'flat' baseline. NAA is almost completely depleted and there is a characteristic pattern of increased glutamine resonances (2.2–2.4 ppm).

Cho/Cr peak-ratio is apparently increased, compared with the normal above, but in this case the impression is created by reduction in Cr intensity (that can only be ascertained from a quantitative spectrum).

The patient with acute hepatic encephalopathy (Fig. 4, spectrum 3, HE) shows peaks in the lipid/lactate region that cannot be reliably interpreted. NAA/Cr is clearly reduced, whereas the cluster of peaks designated Glx is obviously increased. Cho/Cr is if anything slightly less than normal, but the most striking change is the almost complete absence of myoinositol (mI). This also makes the increased α -Glx peaks to the left of mI more easily visible.

The lower spectrum (Fig. 4, spectrum 4, AD), "probable Alzheimer disease," also has a characteristic appearance, with NAA much reduced (NAA/Cr close to 1). Glx is if anything reduced, whereas Cho/Cr is in this case slightly higher than the normal. The prominent mI peak is almost equal to Cr and NAA intensities giving the spectrum its characteristic "flat" appearance.

In each case MRI was essentially normal, and gave little or no diagnostic information, whereas the spectrum is now well established as characteristic for the disease state described.

Normal Brain Development

The evolution of MRS changes in the newborn brain, from *in utero* (in a single near-term fetus) (Heerschap and van den Berg, 1993) to post-partum 300 plus weeks of gestational age, is now well described (Figs. 5 and 6) (Kreis et al., 1993b). The findings add significantly to the information routinely obtained in MRI. Van der Knaap et al. (1993) have correlated the evolution of changes in the ^{31}P and ^1H MRS with the development of myelination. Normative curves for normal development now established for two cerebral locations (Fig. 6) confirm earlier published long-echo time and ^{31}P findings. *Myo*-inositol dominates the spectrum at birth (12 mmol/kg), whereas choline is responsible for the strongest peak in older infants (2.5 mmol/kg). Creatine (plus phosphocreatine) and *N*-acetyl groups (NA, of which the major component is NAA)

TABLE 5. Differential diagnostic uses of magnetic resonance spectroscopy

Metabolite (normal cerebral concentration)	Increased	Decreased
Lactate (Lac) (1 mM; not visible)	often Hypoxia, anoxia, near-drowning, ICH, stroke, hypoventilation (inborn errors of TCA, etc), Canavan, Alexander, hydrocephalus	unknown
N-acetylaspartate (NAA) (5, 10, or 15 mM)	rarely Canavan	often Developmental delay, infancy, hypoxia, anoxia, ischemia, ICH, herpes II, encephalitis, near-drowning, hydrocephalus, Alexander, epilepsy, neoplasm, multiple sclerosis, stroke, NPH, diabetes mellitus, closed head trauma
Glutamate (Glu) or glutamine (Gln) (Glu = ? 10 mM; Gln = ? 5 mM)	Chronic hepatic encephalopathy (HE), acute HE, hypoxia, near-drowning, OTC deficiency	unknown Possibly Alzheimer disease
Myo-inositol (mI) (5 mM)	Neonate, Alzheimer disease, diabetes mellitus, recovered hypoxia, hyperosmolar states	Chronic HE, hypoxic encephalopathy, stroke, tumor
Creatine (Cr) + phosphocreatine (PCr) (8 mM)	Trauma, hyperosmolar, increasing with age	Hypoxia, stroke, tumor, infant
Glucose (G) (~1 mM)	Diabetes mellitus, ? parental feeding (G), ? hypoxic encephalopathy	Not detectable
Choline (Cho) (1.5 mM)	Trauma, diabetes, "white" vs. "gray", neonates, post-liver transplant, tumor, chronic hypoxia, hyperosmolar, elderly normal, ? Alzheimer disease	Asymptomatic liver disease, HE, stroke, nonspecific dementias
Acetoacetate; acetone; ethanol; aromatic amino acids; xenobiotics (propanediol; mannitol)	Detectable in specific settings Diabetic coma; ketogenic diet (Seymour et al., 1998) etc.	

ICH, intracerebral hemorrhage; TCA, tricarboxylic acid cycle; NPH, normal pressure hydrocephalus; OTC, ornithine transcarbamylase.

are at significantly lower concentrations in the neonate than in the adult (Cr ~6 and NAA ~5 mmol/kg). NAA and Cr increase, whereas Cho, and particularly mI decrease during the first few weeks of life (Table 3) (Kreis et al., 1993b). Increased NAA and Cr are determined by gestational age, whereas the falling concentration of mI correlates best with postnatal-age.

Absolute metabolite concentrations depend upon metabolite T_1 and T_2 relaxation. Although T_1 values alter significantly with age for the metabolites NAA, Cr and mI, that for Cho is not altered. T_2 of NAA does seem to show important changes between newborns and adults whereas those of Cr, Cho and mI seem to be unimportant.

Quantitative ^1H MRS is expected to

be of particular value in diagnosis and monitoring of pathology in infants (Van der Knaap et al., 1993), because metabolite ratios are often misleading. This may be particularly useful in that period before myelination is apparent in the developing brain.

Nonspecific cerebral damage in inborn errors of metabolism may consist of disturbance of brain maturation.

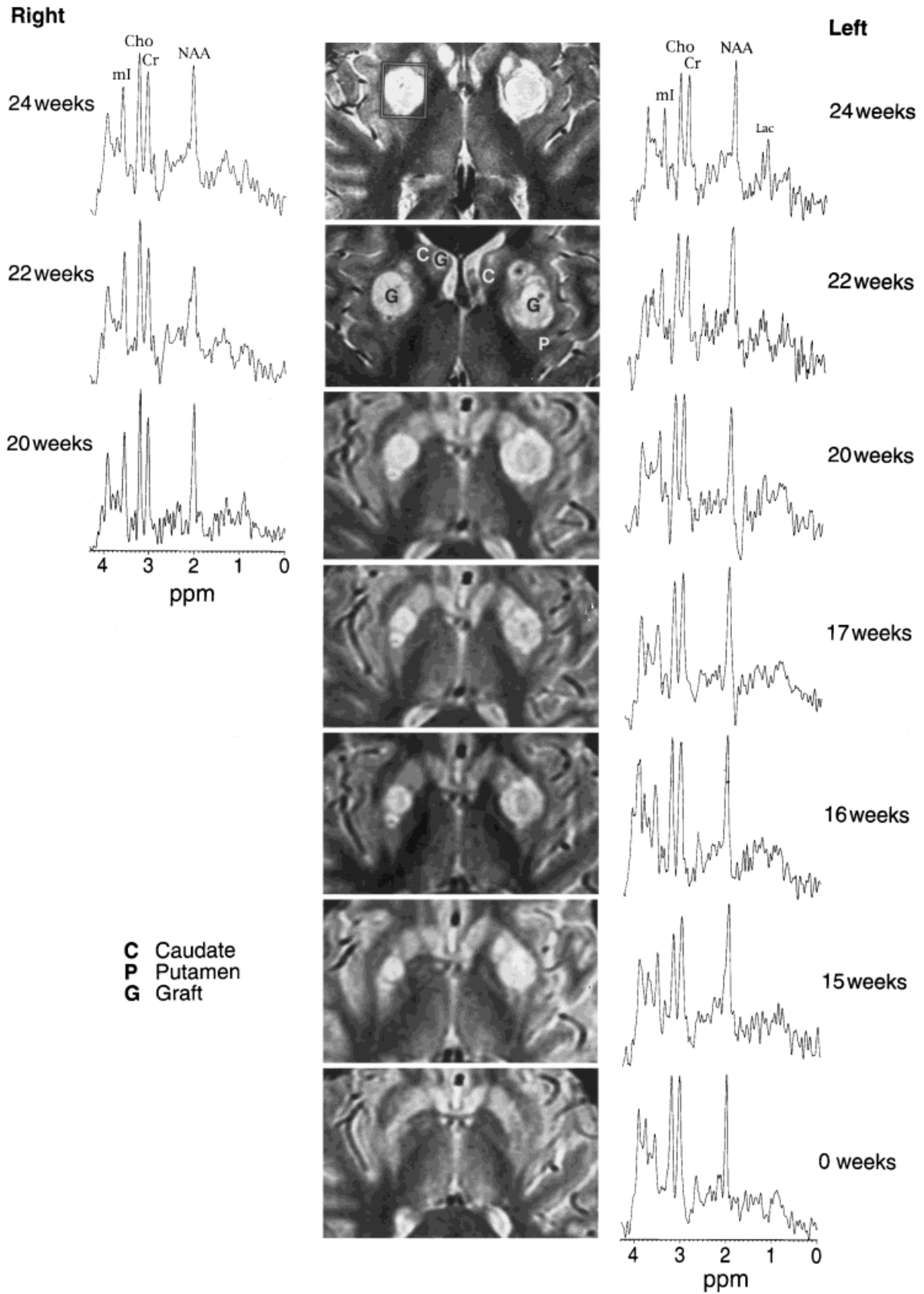
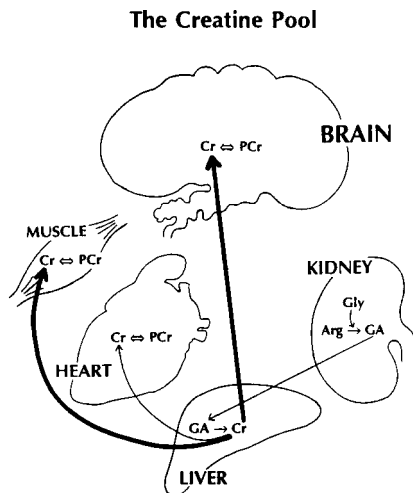


Figure 10. Time course of development of bilateral fetal grafts in a patient with Huntington disease. In ascending order, sequential MRI studies demonstrate the increasing volume of bilateral fetal grafts placed in the putamen and caudate. In the latest examination, a cyst has developed on the left. Localized ¹H MR spectra are depicted for each examination of left and right sided grafts. Peaks identified as NAA, Cr, Cho and ml reflect a near-normal adult (rather than fetal) neuro-chemistry for those well-established neuro-transplants. Corresponding to the developing cyst, lactate is noted in the latest ¹H MR spectrum (top left), and may be an early indicator of graft "failure" (modified from Hoang et al., 1998, with permission of the publisher).



creatine (Cr); phosphocreatine (PCr); arginine (Arg); glycine (Gly); guanidinoacetate (GA)

Figure 11. The creatine pool. Creatine (Cr) synthesis requires participation of kidney and liver. Tissues may express creatine kinase, in which case phosphocreatine (PCr) will be present. Other tissues lack PCr.

tion, demyelination, or neuronal degeneration. In demyelinating disorders, it is primarily the myelin sheath that is lost; secondarily, axonal damage and loss occurs.

In demyelinating disorders, the rarefaction of white matter implies that the total amount of membrane phospholipids per volume of brain tissue decreases. Myelin sheaths consist of condensed membranes with a high lipid content.

Myelination in normal brain commences in the 6th month of fetal development and continues to adult years. Peak myelin production, however, occurs from 30 weeks gestation to 8 months postnatal development with young adult-like myelination observed at age 2 years (Brody et al., 1987). Phospholipids containing ethanolamine (E) and phosphoglycerides containing choline (Cho) are constituents of sphingomyelin and lecithin respectively, both of which are components of the myelin sheath. ¹H decoupled ³¹P MRS ([¹H]-dc³¹P) is able to separate the complex phosphomonoester and diester peaks into their components of phosphoethanolamine (PE), glycerophosphoethanolamine (GPE), phosphatidylcholine (PC) and glycerophosphatidylcholine (GPC). Quantitative [¹H]-dc³¹P can be used to investigate and quantify age-related changes in the choline and

ethanolamine constituents of normal, developing and diseased human brain in vivo (Bluml et al., 1998a,b) (see discussion of hepatic encephalopathy in Box 2).

Using a modified PRESS (TE = 12 ms, TR = 3 s) sequence, and [PCr]

obtained from each quantitative non-decoupled ³¹P MRS as an internal reference, quantification of [PE], [PC], [GPE], [GPC] shows the age-related changes of membrane metabolites in vivo. The [¹H]-dc³¹P spectra from controls of different ages show clear

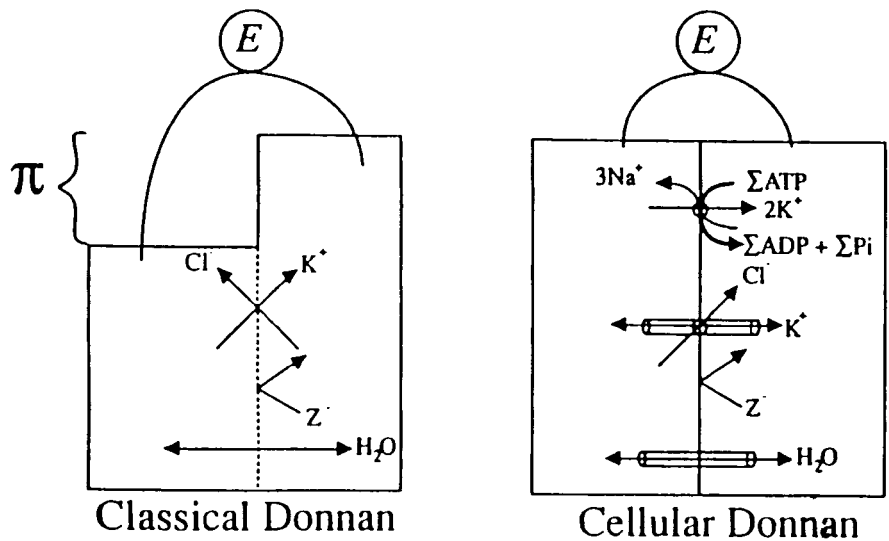
Cr

1. Single T₂ species
2. Rapid exchange
3. Invisible pool?—not likely (8.0 vs 8.6 mM)
4. Neuron vs glial marker—(8.0 vs 6.3 mM; GM vs WM; unlikely)

3rd “force” controls [Cr]

- (a) Enzyme equilibrium: early hypoxia, no change in [Cr + PCr]; Cr/PCr ↑
- (b) Biosynthesis in liver and kidney: liver disease ↓ [Cr]
- (c) Gibbs-Donnan equilibrium [Cr] ↑ or ↓

Gibbs-Donnan Equilibrium Control Cell Volume and Biochemistry in Brain



$$[\Sigma P_i] = \frac{[\Sigma 3PG] [\Sigma LACT] [\Sigma P-Cr] [H^+]}{[\Sigma DHAP] [\Sigma PYR] [\Sigma Creatine]} \times \frac{K_{LDH} \times K_{CK} \times K_{TPI}}{K_{G+G}}$$

1. Electrolytes, metabolites and osmolytes “interact.”
2. Metabolites (even PCr) might be osmolytes.

ERGO: We will observe reversible changes in [Cr] and [NAA]

Figure 12. Creatine: Gibb-Donnan Equilibrium. Modified from R.L. Veech, with permission.

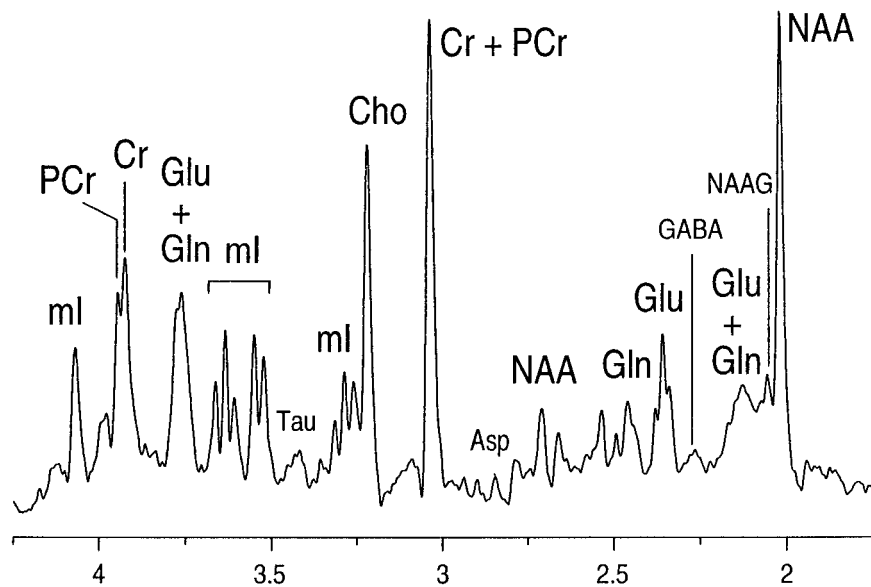


Figure 13. Ultra high field resolves "choline" region in vivo. ^1H NMR spectrum acquired from a 1 ml volume lateral to the ventricle in dog brain at 9.4 Tesla. Processing consisted of zero-filling, 3 Hz Lorentz-to-Gauss lineshape conversion and FFT. Peaks were tentatively assigned based on dominant constituent and published chemical shifts. Courtesy of Drs. R. Gruetter and I. Tkac.

differences related to age. The largest change is observed in [PE] that is initially high and decreases to adult levels by about age 10 years. [PC] is also high in the neonate and decreases to young adult concentrations by about age 4 years. Phosphocreatine (PCr) concentrations increase and reach adult levels at age 4. [GPE] and [GPC] show a slight generally increasing trend with age (Figs. 7 and 8)

Pathology

Comparing MR spectra with those from relevant age-matched normal subjects, a number of examples of inappropriate development have been identified. *Canavan disease* (Fig. 9 left), a disorder arising from aspartoacylase deficiency. It is presented in proton MRS (see Fig. 18B for sequential proton MRS for treatment monitoring in this patient) with highly elevated NAA, elevated ml and reduced total Cr and Cho. Additional information about the pathophysiology of this rare inborn error is obtained by ^1H - ^{31}P MRS, the membrane metabolites PC, GPE, and GPC as well as the high energy metabolites PCr and ATP appearing to be reduced.

A patient (Fig. 9B) initially diagnosed with and treated for hydrocephalus did not do well clinically and

showed abnormal myelination in follow-up exams. GPC was found to be reduced whereas PCr appears to be elevated.

A patient (Fig. 9C) with amino acid inborn error disease (*glutaric aciduria II*) showed elevated GPE, GPC, and PCr.

In consolidated *late hypoxic injury*, increased GPE, GPC, and PCr may reflect a partial volume effect of increased glial cells density (Fig. 9D).

In all patients information separately acquired with proton MRS is consistent with ^1H - ^{31}P MRS findings insofar as total Cr (= free Cr + PCr) and total Cho (GPC + PC + minor contributions from other metabolites) parallels changes in PCr or GPC and PC (see Fig. 9 left panel).

Rapid changes in [PE] and [PC], which are important precursors of phospholipids, may be related to the high rate of synthesis of membranes and myelin in the young developing brain.

WHAT HAVE WE LEARNED FROM NEUROSPECTROSCOPY?

Table 5 summarizes abnormalities observed by ^1H MRS in diseases. When observing neuropathological events through MRS, there seems to be a rather limited range of metabolic

changes in response to disease. Tumor, MS, stroke, inflammation, and infections may produce very similar patterns of change. This is not surprising and should not be condemned as lack of specificity. Rather, it should teach us more about the brain's response to injury and its prevention and repair.

N-Acetylaspartate (NAA)

Most observations with ^1H MRS strongly support the original formulation of NAA as a "neuronal marker." This simple conclusion, however, must be modified in some particulars. In addition to neurons, there is evidence that NAA is found in a precursor cell of the oligodendrocyte. The time-course of appearance of NAA in human embryology remains unknown, but the best estimate is that NAA biosynthesis may begin in the middle trimester, i.e., it is not dependent upon the existence of MRI-visible myelin, which is only slowly added to the brain in the months after birth. Furthermore, the finding of approximately equal concentrations of NAA in white and gray matter of the human brain makes it inescapable that NAA is also a component of the axon or the axonal sheath in man. In addition to NAA, there is good evidence now for the existence of NAAG in human (as well as animal) brain, with the preponderance in white matter, and posterior and inferior regions of adult brain, especially the cerebellum.

Human pathobiology also supports the idea of NAA as a neuronal marker, loss of NAA being generally an accompaniment of diseases in which neuronal loss is documented. Glioma, stroke, the majority of dementias, and hypoxic encephalopathy all show loss of NAA.

That NAA is an "axonal marker" too, is supported by the loss of NAA in many white matter diseases (leukodystrophies of many kinds have been studied), in MS plaques and in white matter in hypoxic encephalopathy.

If NAA is a neuronal marker, can we ever expect to see recovery of NAA in practice? A clear example of neuronal recovery or regeneration is provided by the fetal neural transplant into adult human brain (Hoang et al., 1997, 1998). Convincing evidence of

SCHEMATIC DIAGRAM SHOWING INOSITOL AND INOSITOL POLYPHOSPHATE METABOLISM

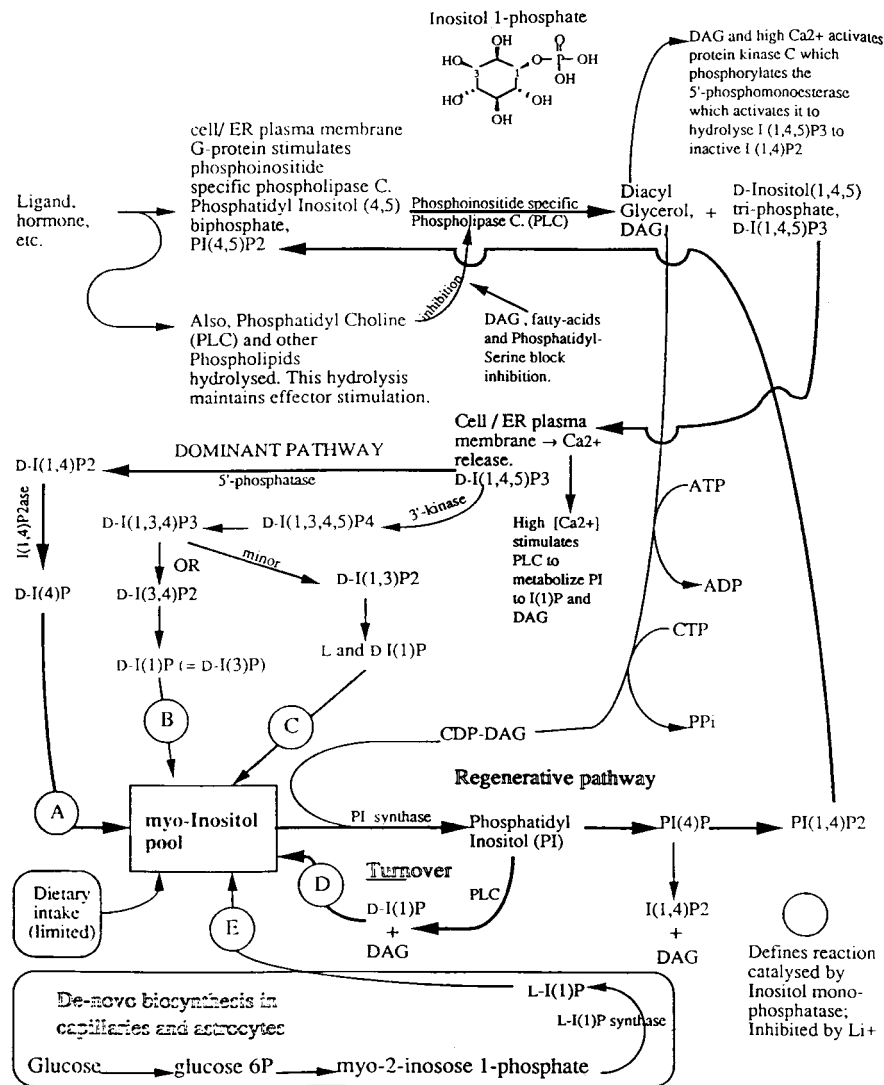


Figure 14. Reactions involving *myo*-Inositol (ml).

the presence of NAA in the grafted region of the putamen is provided by sequential examinations in such a patient, by means of localized ^1H MRS (Fig. 10). Most other examples proposed are perhaps best understood not as evidence of neuronal recovery (still to be viewed as unlikely), but as one of five possible alternatives:

Axonal recovery, after a less than lethal insult to the neuron, as for example in MS plaques, or in the rare MELAS syndrome.

An "artifact" of cortical atrophy. Thus, as neuronal death occurs, the consolidation of surviving brain tissue is well

documented by neuropathological studies, and by cortical atrophy on MRI. MRS that determines local ratios or even concentrations of NAA will record a real increase in the local concentration of this metabolite.

Survival (or recovery) of a peak at 2.01 ppm in the proton spectrum may not be due to NAA or NAAG, but to several other metabolites that contribute to this spectral region. A small decrease in the NAA peak in diabetes mellitus may be explained better in terms of another metabolite.

NAA appears also to be a re-

versible cerebral osmolyte, increasing or decreasing in response to hyper-osmolar states, and decreasing noticeably in hypo-osmolar states, such as sodium depletion and possibly hydrocephalus (Bluml et al., 1997).

Slow NAA Resynthesis (Moreno et al., unpublished observations).

Creatine (Cr) and Phosphocreatine (PCr)

We know that, in human brain at least, these two compounds, which are in rapid chemical, enzymatic exchange, represent a single T_2 species. MRS estimates 8 mM Cr + PCr in human gray matter, compared with published values of 8.6 mM for rapidly frozen rat brain. Cr concentration in human gray matter significantly exceeds that measured in white matter, in contrast to the results of tissue culture studies, in which Cr seems to be more related to astrocytes than to neurones (Flögel et al., 1995).

As with NAA, MRS studies have thrown very interesting light upon the factors that might control Cr + PCr in the human brain. In addition to the well-known regulation by enzyme equilibrium that permits a presumably crucial role of PCr in energetics of ATP synthesis, two new concepts have emerged. The first is that cerebral Cr is controlled by distant events, due to the complex biosynthetic pathway through liver and kidney enzymes. Before Cr can be available for transport to the brain it must be synthesized (Fig. 11). Absolute cerebral [Cr] falls in chronic liver disease, and recovers after liver transplantation. Even more striking is the recent discovery of a new human inborn error of Cr biosynthesis that manifests as absence of cerebral Cr from the proton spectrum, which can be corrected by dietary administration of creatine (Hanefeld et al., 1993).

The third method of regulation of cerebral Cr content is surprising, in view of the crucial nature of cerebral energy conservation. This is the marked modification of cerebral Cr by osmotic (Donnan) forces, increased in hyperosmolar states and decreased in the very common setting of hypo-osmolar states due to sodium depletion. The explanation for this apparent

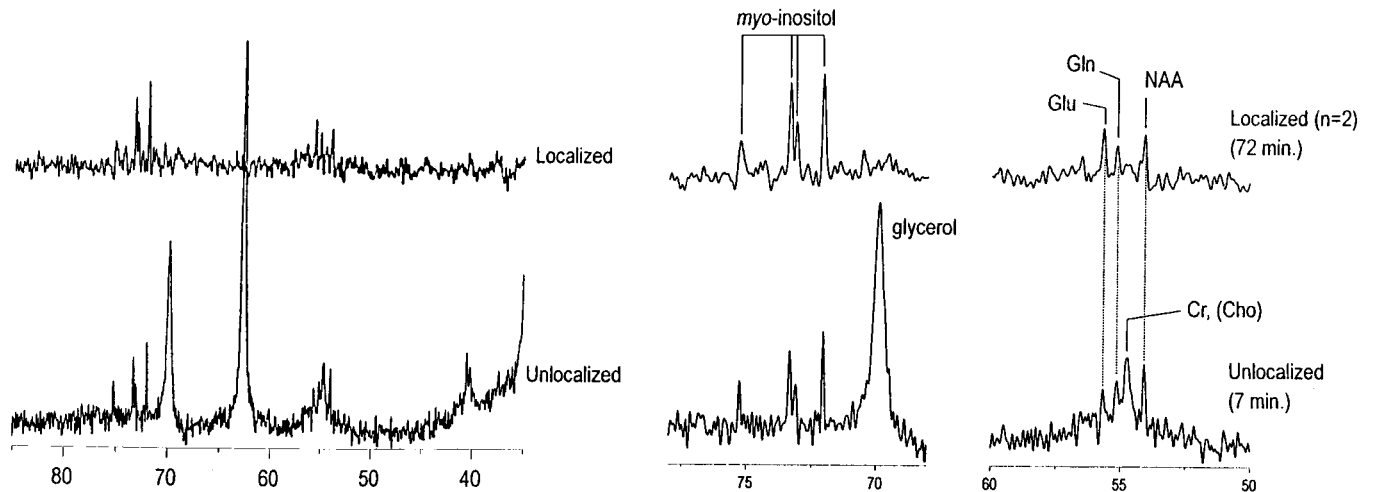


Figure 15. Natural abundance proton decoupled ^{13}C MRS. Shown is a comparison of localized (top) and unlocalized (bottom) natural abundance ^{13}C MRS at 4 Tesla. Peaks from *myo*-inositol at 72.0, 73.0, 73.3, and 75.1 ppm, as well as the C2 glutamate at 55.7, C2 glutamine at 55.1 ppm, and C2 NAA at 54.0 ppm can readily be detected. Peaks from creatine and choline overlap at 54.7 ppm and are eliminated from the localized spectrum by the polarization transfer technique used to acquire the localized spectrum (reproduced from Gruetter et al., 1996 with permission of the publisher).

over-riding of the all-important enzyme equilibrium (Gibbs) forces is probably the same as that recently discovered for the mammalian heart and for cancer cells. Namely, Gibbs equilibrium and Donnan equilibrium are very closely linked. When all equilibria are interdependent, then the total $[\text{Cr} + \text{PCr}]$ may rise or fall to maintain the osmotic equilibrium. We presume, but cannot tell from ^1H MRS alone, that even under these circumstances, the ratio of PCr/Cr continues to comply with the over-riding requirements of the thermodynamic equilibrium between PCr and ATP (Fig. 12).

An interesting example of this complexity is the observation that the concentration of $[\text{Cr}]$ and of $[\text{PCr}]$ is increased in the late-hypoxic-encephalopathy brain (Fig. 9D). This secondary effect is presumably a reflection of a new steady state, in which creatine kinase equilibrium is maintained, but the residual cell-population ("gliosis") is defined by a higher total creatine content (Bluml et al., 1998a).

Cholines (Cho)

A number of new ideas concerning the choline resonance and its constituent metabolites have emerged from clinical studies. Although theoretically associated with myelin, the choline concentration in cerebral white matter is not much higher than that in gray matter, even though this is the im-

pression one gains from constantly seeing ^1H spectra, in which Cho/Cr is much higher and nearer to 1.0 in short echo-time spectra of white matter. The explanation lies in the difference of $[\text{Cr}]$ concentration between the two locations, the $[\text{Cr}]$ concentration being approximately 20% higher in gray matter. Thus, the $[\text{Cho}]$ is only a little higher, 1.6 mM in white matter and 1.4 mM in gray matter. The choline head-groups of phosphatidylcholine contribute hardly at all to the proton spectrum of the human brain *in vivo* since the total of free choline, plus phosphoryl choline plus glycerophosphoryl choline determined by chemical means in human brain biopsies and post-mortem samples is very close to 1.5 mM.

As with Cr , osmotic events are among the many local and systemic events that alter its concentration in brain. The finding that many focal, inflammatory and hereditary diseases result in increased choline concentration has led to the speculation that these metabolites represent breakdown products of myelin. Conversely, the finding that several systemic disease processes also modify cerebral choline indicates that biosynthesis and hormonal influences outside the brain, possibly in the liver, can markedly alter the composition and concentration of the choline peak. These remain to be elucidated. Although proton spectroscopy offers little hope

of distinguishing the different components, (*in vivo* ^1H MRS at very high field (e.g., 9 Tesla) is showing some promise (Fig. 13), proton decoupled phosphorus spectroscopy undoubtedly can do so, giving the opportunity to use disease processes to further understand these interesting metabolites. Figure 1B (modified from Prof. D. Leibfritz) integrates a number of these ideas concerning cerebral choline and ethanolamine metabolites, which are directly accessible through MRS.

Myo-Inositol (mI) and Scyllo-Inositol (sI)

Some remarkable facts have emerged concerning this simple sugar-alcohol that was rediscovered with the advent of short TE *in vivo* human brain spectroscopy. Its concentration fluctuates more than any of the other major compounds detected in the proton spectrum, over 10-fold, from the three-times adult normal values in newborn infants and hypernatremic states, to almost zero, in hepatic encephalopathy. mI has been recognized as a cerebral osmolyte since 1990, and its cellular specificity is believed to be as an astrocyte 'marker.' Like Cho , mI has been labeled as a breakdown product of myelin (because it is seen at apparently increased concentration in MS plaque, HIV infection and metachromatic leukodystrophy). But

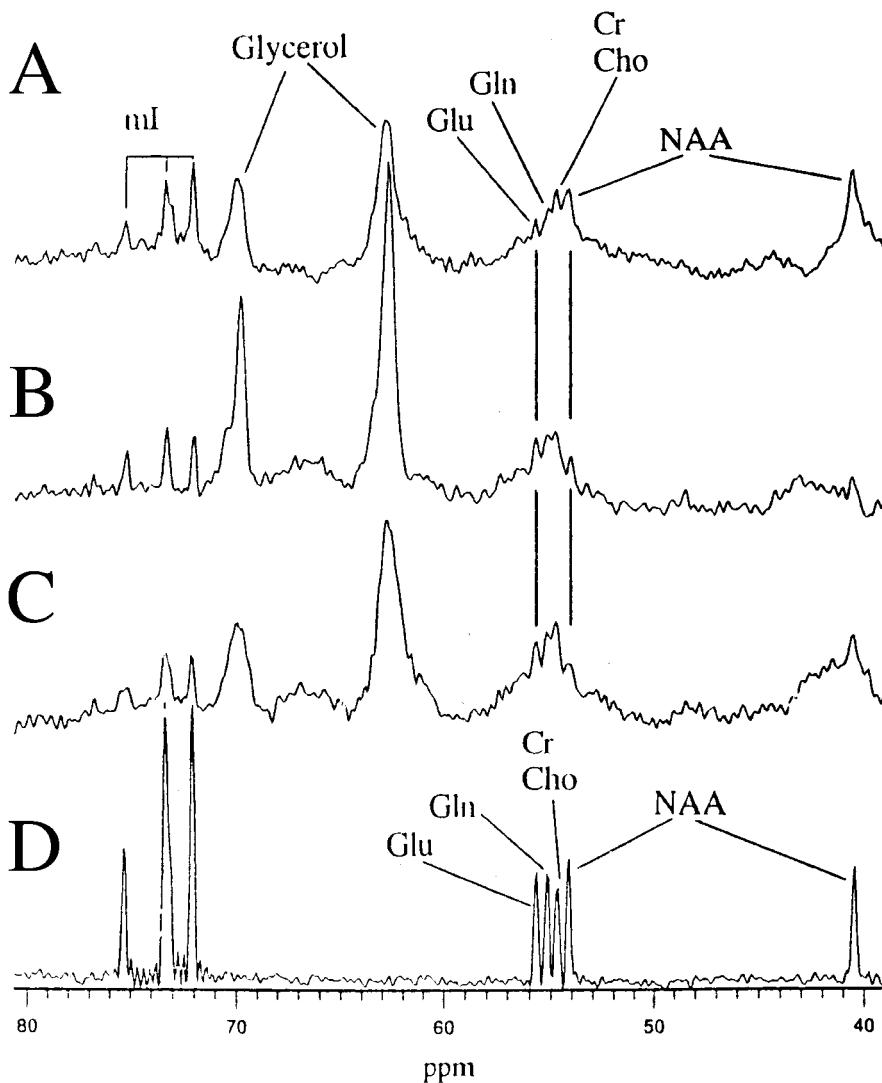


Figure 16. Natural abundance proton-decoupled ^{13}C MRS in Canavan disease acquired on a Clinical Scanner at 1.5 T. Details of in vivo $\{^1\text{H}\}$ - ^{13}C spectra from a child diagnosed with Canavan Disease (A), 7 months and 3 years old controls (children with unrelated diseases) (B,C) aligned with a spectrum from a model solution (D). mI at 72.1, 73.3, and 75.3 ppm and NAA at 40 and 54 ppm can be clearly identified. Peaks at 54.6 and 55.2 ppm are consistent with Cr/Cho and Gln. Note that Glu at 55.7 ppm is obviously depleted in Canavan disease when compared with control spectra. NAA and mI resonances appear to be elevated in Canavan disease, confirming ^1H MRS results. Glycerol peaks at 62.9 ppm and 69.9 ppm are well decoupled (reproduced from Bluml, 1998 with permission of the publisher).

the evidence is particularly indirect on this point. Despite attempts to confine the role of mI to that of a chemically inert osmolyte or cell marker, it is important to remember that mI is at the center of a complex metabolic pathway that contains among other products the inositol-polyphosphate messengers, inositol-1-phosphate, phosphatidyl inositol, glucose-6-phosphate and glucuronic acid (Fig. 14). Any or all of these products may be involved in diseases that result in marked alterations in mI or sI concentration. The differentiation of inositol phosphate

from mI that is difficult to achieve with ^1H MRS, is likely to be achieved by a combination of proton decoupled ^{31}P MRS and natural abundance ^{13}C MRS (Ross et al., 1997).

Glutamine (Gln) and Glutamate (Glu)

Provided care is taken, and the appropriate sequences applied, even at 1.5 T, the two amino acids that contribute to the spectral regions 2.2–2.4 and 3.6–3.8 ppm can be separated. Glutamine, particularly when present at

elevated concentrations can be determined with some precision. Even better separation is achieved at 2.0 T, when glutamate can be unequivocally identified and quantified. It is glutamine concentration, rather than that of glutamate that seems to respond to disease. Increased cerebral glutamine concentration occurs in many settings, from Reyes syndrome, and hepatic encephalopathy to hypoxic encephalopathy. It is the latter case that seems contrary to popular neurochemical theory.

The determination of in vivo cerebral glutamate and glutamine (Glx) concentrations using ^1H MRS is compromised, however, by the complex spectral appearance of glutamate/glutamine due to J-coupling. Further, other metabolites contributing to the signal at the chemical shift of glutamate/glutamine render their quantitation difficult. Studies demonstrated the potential of natural abundance in vivo ^{13}C for direct determination of cerebral metabolites at 2.1 and 4 T experimental systems (Fig. 15) (Gruetter et al., 1994, 1996). In a recent study, however, it was shown that even on a 1.5 Tesla clinical scanner, glutamate and glutamine can be separated from each other, and natural abundance ^{13}C MRS provides enough S/N ratio for their in vivo quantitation (Fig. 16) (Bluml, 1998).

A much closer look at glutamate turnover is achieved through the use of either ^{13}C or ^{15}N MRS (the former in human brain). Mason et al. (1995) and Gruetter et al. (1994) determined the rates of the TCA cycle, glucose consumption, glutamate formation from 2-oxoglutarate (Fig. 17) and finally the rate of glutamine synthesis (GS) in vivo. Their data is consistent with the long held view of two glutamate compartments. By selecting the appropriate starting substrate, acetate vs. glucose (Bluml et al., 2001), ^{13}C MRS permits direct assay of the in vivo astrocyte and neuronal glutamate turnover rates in the human brain.

Although no explanation is yet available for the accumulation of glutamine rather than glutamate in hypoxic brain, the work of Kanamori and Ross (1997) with ^{15}N MRS offers some clues (Fig. 1D). Thus, the rate of PAG, the sole pathway of glutamine

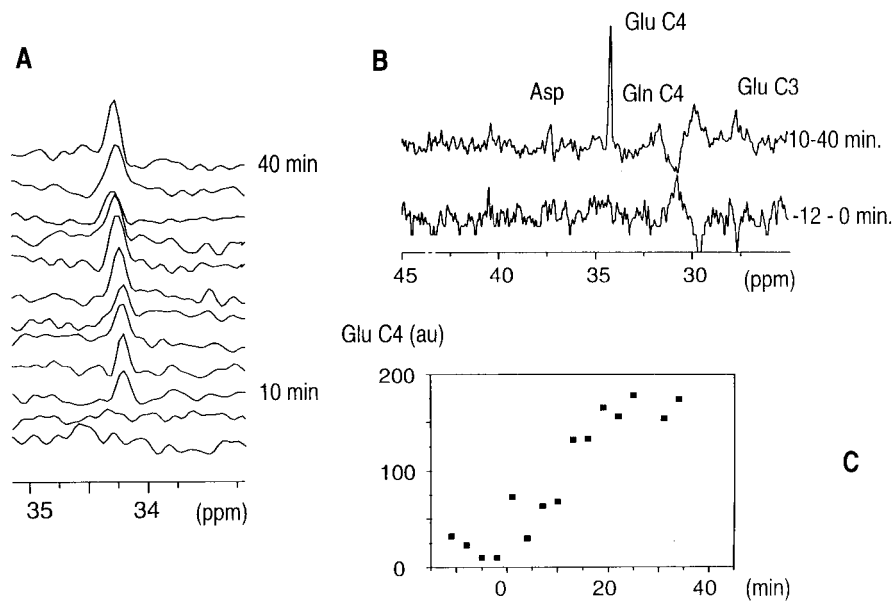


Figure 17. In vivo proton-decoupled ^{13}C MRS with ^{13}C -labeled glucose infusion at 4T. ^{13}C enriched glucose infusion studies allow the determination of glycolysis and TCA cycle flux rates in vivo. Direct ^{13}C NMR detection of label accumulation in a 22.5 ml volume in the visual cortex was measured by Greutter et al. (1996) at 4 T. **A:** Stack plot with 3 min time resolution of the region containing the Glu C4 resonance at 34.2 ppm. **B:** Pre-infusion spectra with data accumulation extended to 12 min and spectrum acquired within 30 min after start of infusion. **C:** Time course of the C4 glutamate resonances after infusion of $1\text{-}^{13}\text{C}$ -labeled glucose. Courtesy of Dr. G. Mason.

breakdown to glutamate, is under tight metabolic control in the (rat) brain. Because there is a cycle converting glutamate to glutamine and back, it may be that PAG holds the answer to the regulation of cerebral glutamate concentration in hypoxia. On the horizon are new insights through ^{13}C and ^{15}N ; Figures 1C,D illustrate the present state of our knowledge of in vivo flux rates, measured in the brain.

MULTINUCLEAR MRS

Solving a Problem: Multinuclear MRS of the Brain In Vivo

With the extraordinary family of MRS techniques now available to the human neuroscientist, we await an explosion of new knowledge. MRS is so rich in information, and conveniently correlated with MRI, fMRI and related procedures, that the concept of “one-stop-shopping” is close at hand. Within MRS, combining carefully quantified multi-nuclear studies can expand the utility of the equipment.

This approach is illustrated by the example of *Canavan disease*, a defi-

ciency of aspartoacylase that results in hypomyelination with megaloccephaly, blindness and spasticity, and death within the first few years of life. The potential of multi-nuclear in vivo MR spectroscopy is illustrated on a single patient who underwent a series of noninvasive MRS examinations (see Fig. 18 and also Fig. 2 of the Supplementary Material [INSERT URL]). Regions of different cell type composition (e.g., gray vs. white matter) were readily identified on MRI. Localized ^1H MRS provided quantitation of brain water and the neuronal marker NAA (Fig. 18B). Reduced aspartoacylase activity in this disease is expected to result in an elevation of NAA, readily observed by ^1H MRS. Sequential ^1H MRS further offers the possibility of monitoring therapy. Other abnormalities such as low cerebral Cho, high mI, excess of sI, and a subtle reduction of total Cr are observed as well.

Additional information about the pathophysiology of this rare inborn error was obtained by proton-decoupled ^{31}P MRS insofar as the membrane metabolites PC, GPE, and GPC appear to be reduced (Fig. 18C). Alter-

ations in those putative membrane metabolism markers may reflect delayed or abnormal myelination. Total Cho from ^1H MRS can be correlated with myelin metabolite and osmolyte determinations from proton-decoupled ^{31}P MRS. A reduction in cerebral PCr confirms low total Cr (= free Cr + PCr) from ^1H MRS. The significance of the slightly decreased ATP is uncertain.

Natural abundance $[^1\text{H}]\text{-}^{13}\text{C}$ MRS confirmed elevated NAA and mI and detected a striking reduction of glutamate (Fig. 18D). This may be a result of the sequestration of aspartate in NAA and the reduction of free aspartate. $1\text{-}^{13}\text{C}$ -glucose MRS demonstrated a 60% reduced rate of NAA synthesis in Canavan disease compared to control (not shown). In summary, as demonstrated in this rare inborn error disease, in vivo MRS can be used to quantify and monitor metabolic abnormalities and may provide significant contributions to our understanding of human neuropathophysiology.

Phenotyping Knock-Out Mouse Models of Neurological Disease by In Vivo MRS

Although our emphasis has been on human neurochemistry (an obvious need, given the inaccessibility of the brain for in vivo analysis) there has been no shortage of applications of MRS to experimental animals. Perhaps the most important in the future will be studies of transgenic and knock-out mice. This rapidly expanding research tool poses the broad problem of phenotyping to confirm that the deleted gene really does regulate the anticipated metabolic pathway. MRS studies of knock-outs or transgenics energy metabolism, diabetes, and neurological disorders such as Huntington and Alzheimer disease are to be found in the literature; recent advances are reviewed in Beckmann et al. (2001).

CONCLUSIONS

Studies in neuroscience have generated myriad biochemical questions, many of which are beyond the scope of in vivo MRS. The ideal question involves global (or at least “million-neuron”) events and millimolar

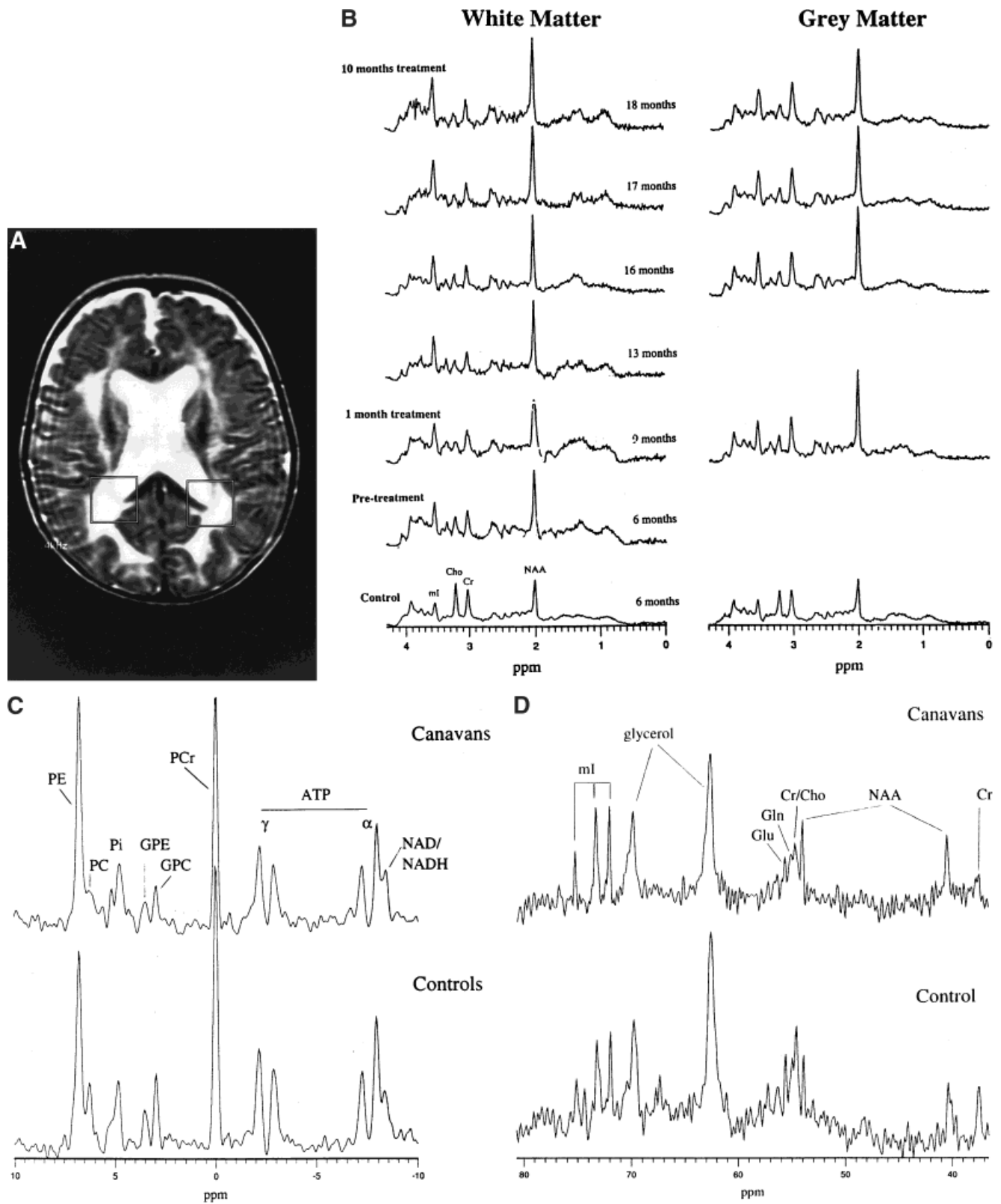


Figure 18. Multi-nuclear MRS of the brain in vivo: Canavan disease. A Canavan disease patient underwent ^1H , $\{^1\text{H}\}$ - ^{31}P , and $\{^1\text{H}\}$ - ^{13}C MRS at a standard clinical 1.5 T scanner equipped with a second rf channel. Quantitative information is transferable from one assay to the next, greatly enhancing the study. **A:** Standard MRI to detect anatomical abnormalities and to identify regions or volumes of interest (VOI). **B:** Sequential ^1H MRS of white and gray matter, from 6 to 18 months. **C:** By $\{^1\text{H}\}$ - ^{31}P MRS the membrane metabolites PC, GPE, and GPC appear to be reduced. A small reduction in cerebral PCr and ATP was also detected. **D:** Natural abundance $\{^1\text{H}\}$ - ^{13}C MRS shows elevated NAA and ml, and reduction of glutamate.

changes in concentration or flux, on time-scales of minutes rather than seconds. By applying these three filters at the outset (volume, concentration, and time), the likelihood of a successful outcome for the early studies is increased.

As a new technology, MRS is perhaps less bound by rules of "hypothesis-driven" research. Witness the unexpected inventions of fMRI, diffusion tensors, magnetization transfer, relaxation time, and nuclear-Overhauser-effect determination. In vivo MRS brings great benefits to neuroscience, not least because studies previously only conceivable in experimental animals, become extremely inviting in man.

In vivo MRS brings great benefits to neuroscience, not least because studies previously only conceivable in experimental animals become extremely inviting in man.

ACKNOWLEDGMENTS

Thanks to Ms. Mary Muñoz who typed the manuscript and Jeannie Tan who prepared many of the figures. We are grateful to our colleagues, Drs. Roland Kreis, Thomas Ernst, Else Rubæk Danielsen, Kay Seymour, Jong-Hee Hwang, Alex Lin, Frederick Shic, Angel Moreno and Cat-Huong Nguy for permission to quote recent or unpublished work. The MRS Unit at HMRI received financial support from the Rudi Schulte Research Institute and from NIH and the Board of HMRI, without which this manuscript would not have been possible. Figures are reproduced with permission. B.D.R. and S.B. are also Visiting Associates at the California Institute of Technology.

LITERATURE CITED

- Ackerman JJH, Bore PJ, Wong GG, Gadian DG, Radda GK. 1980. Mapping of metabolites in whole animals by ^{31}P NMR using surface coils. *Nature* 283:167-170.
- Badar-Goffer RS, Ben-Yoseph O, Bachelard HS, Morris PG. 1992. Neuronal-glia metabolism under depolarizing conditions. *Biochem J* 282:225-230.
- Barker PB, Soher BJ, Blackband SJ, Chatham JC, Mathews VP, Bryan RN. 1993. Quantitation of proton NMR spectra of the human brain using tissue water as an internal concentration reference. *NMR Biomed* 6:89-94.
- Beckmann N, Müggler T, Allegrini PR, Laurent D, Rudin M. 2001. From anatomy to the target: contributions of magnetic resonance imaging to pre-clinical pharmaceutical research. *Anat Rec (New Anat)* 265:85-100.
- Bluml S. 1999. In vivo quantification of cerebral metabolite concentrations using natural abundance ^{13}C MRS at 1.5 Tesla. *J Magn Reson* 136:219-225.
- Bluml S, McComb JG, Ross BD. 1997. Differentiation between cortical atrophy and hydrocephalus using ^1H MRS. *Magn Reson Med* 37:395-403.
- Bluml S, Moreno A, Ross B. 2001. ^{1-13}C glucose magnetic resonance spectroscopy of pediatric and adult brain disorders. *Proc Int Soc Mag Reson in Med* (in press).
- Bluml S, Seymour K, Ross BD. 1999. Developmental changes in choline and ethanolamine containing compounds measured with proton decoupled ^{31}P MRS in vivo human brain. *Mag Reson Med* 42: 643-654.
- Bluml S, Zuckerman E, Tan J, Ross BD. 1998. Proton-decoupled ^{31}P magnetic resonance spectroscopy reveals osmotic and metabolic disturbances in human hepatic encephalopathy. *J Neurochem* 71:1564-1576.
- Bottomley PA. 1987. Spatial localization in NMR spectroscopy in vivo. *Ann NY Acad Sci* 508:333-348.
- Bottomley PA, Foster TB, Darrow RD. 1984. Depth-resolved surface spectroscopy (DRESS) for in vivo ^1H , ^{31}P and ^{13}C NMR. *J Magn Reson* 59:338-342.
- Bottomley PA, Hart HR, Edelstein WA, Schenck JF, Smith LS, Leue WM, Mueller OM, Redington RW. 1983. NMR imaging/spectroscopy system to study both anatomy and metabolism. *Lancet* 1:273-274.
- Brody BA, Kinney HC, Kloman AS, Giles FM. 1987. Sequence of central nervous system myelination in human infancy: an autopsy study of myelination. *J Neuropathol Exp Neurol* 46:283.
- Brown TR, Kincaid BM, Ugurbil K. 1982. NMR chemical shift imaging in three dimensions. *Proc Natl Acad Sci USA* 79: 3523-3526.
- Cady EB, Costello AM, Dawson MJ, Delpy DT, Hope PL, Reynolds EO, Tofts PS, Wilkie DR. 1983. Non-invasive investigation of cerebral metabolism in newborn infants by phosphorus nuclear magnetic resonance spectroscopy. *Lancet* 1:1059-1062.
- Christiansen P, Henriksen O, Stubgaard M, Gideon P, Larsson HBW. 1993. In vivo quantification of brain metabolites by means of ^1H MRS using water as an internal standard. *Magn Reson Imaging* 11:107-118.
- Danielsen ER, Henriksen O. 1994. Quantitative proton NMR spectroscopy based on the amplitude of the local water suppression pulse. Quantification of brain water and metabolites. *NMR Biomed* 7:311-318.
- Ernst T, Hennig J. 1994. Observation of a fast response in functional MR. *Magn Reson Med* 32:146-149.
- Ernst T, Kreis R, Ross BD. 1993a. Absolute quantitation of water and metabolites in the human brain. Part I: compartments and water. *J Magn Reson* 102:1-8.
- Ernst T, Lee JH, Ross BD. 1993b. Direct ^{31}P imaging in human limb and brain. *J Comput Assist Tomogr* 17:673-680.
- Flögel U, Niendorf T, Serkova N, Brand A, Henke J, Leibfritz D. 1995. Changes in organic solutes, volume, energy state, and metabolism associated with osmotic stress in a glial cell line: a multinuclear NMR study. *Neurochem Res* 20:793-802.
- Frahm J, Bruhn H, Gyngell ML, Merboldt K-D, Hänicke W, Sauter R. 1989. Localized proton NMR spectroscopy in different regions of the human brain in vivo. Relaxation times and concentrations of cerebral metabolites. *Magn Reson Med* 11:47-63.
- Frahm J, Merboldt K-D, Hänicke W. 1987. Localized proton spectroscopy using stimulated echoes. *J Magn Reson* 72:502-508.
- Frahm J, Michaelis T, Merboldt K-D, Bruhn H, Gyngell ML, Hänicke W. 1990. Improvements in localized proton NMR spectroscopy of human brain. Water suppression, short echo times, and 1 ml resolution. *J Magn Reson* 90:464-473.
- Frahm J, Michaelis T, Merboldt KD, Hänicke W, Gyngell ML, Chien D, Bruhn H. 1989. Localized NMR spectroscopy in vivo: progress and problems. *NMR Biomed* 2:188-195.
- Greenman RL, Axel L, Lenkinski RE. 1998. Direct imaging of phosphocreatine in the human myocardium using a RARE sequence at 4.0 T. *Proceedings of the 6th International Society for Magnetic Resonance in Medicine*. Sydney, Australia: 1922.
- Gruetter R, Adriany G, Merkle H, Anderson PM. 1996. Broadband decoupled, ^1H -localized ^{13}C MRS of the human brain at 4 Tesla. *Magn Reson Med* 36: 659-664.
- Gruetter R, Mescher M, Kirsch J, et al. 1997. ^1H MRS of neurotransmitter GABA in humans at 4 Tesla. *Proceedings of the 5th International Society for Magnetic Resonance in Medicine*. Vancouver, Canada: 1217.
- Gruetter R, Novotny EJ, Boulware SD, Mason GF, Rothman DL, Shulman GI, Pritchard JW, Shulman RG. 1994. Localized ^{13}C NMR spectroscopy in the human brain of amino acid labeling from D-[^{1-13}C]glucose. *J Neurochem* 63:1377-1385.

- Gyngell ML, Busch E, Schmitz B, Kohno K, Back T, Hoehn-Berlage M, Hossman KA. 1995. Evolution of acute focal cerebral ischemia in rats observed by localized ^1H MRS, diffusion weighted MRI and electrophysiological monitoring. *NMR Biomed* 8:206–214.
- Hamilton PA, Hope PL, Cady EB, Delpy DT, Wyatt JS, Reynolds EOR. 1986. Impaired energy metabolism in brains of newborn infants with increased cerebral echodensities. *Lancet* 1:1242–1246.
- Hanefeld F, Holzbach U, Kruse B, Wilichowski E, Christen HJ, Frahm J. 1993. Diffuse white matter disease in three children: an encephalopathy with unique features on magnetic resonance imaging and proton magnetic resonance spectroscopy. *Neuropediatrics* 24:244–248.
- Hanstock CC, Rothman DL, Prichard JW, Jue R, Shulman R. 1988. Spatially localized ^1H NMR spectra of metabolites in the human brain. *Proc Natl Acad Sci USA* 85:1821–1825.
- Heerschap A, van den Berg P. 1993. Proton MR spectroscopy of the human fetus in utero. *Proceedings of the 12th Society of Magnetic Resonance in Medicine*. New York: 318.
- Hennig J, Pfister H, Ernst T, Ott D. 1992. Direct absolute quantification of metabolites in the human brain with in vivo localized proton spectroscopy. *NMR Biomed* 5:193–99.
- Hetherington HP, Newcomer BR, Pan JW. 1998. Measurements of human cerebral GABA at 4.1 T using numerically optimized editing pulses. *Magn Reson Med* 39:6–10.
- Hoang T, Dubowitz D, Bluml S, Kopyov OV, Jacques D, Ross BD. 1997. Quantitative ^1H MRS of neurotransplantation in patients with Parkinson and Huntington disease. 27th Annual Meeting, Society for Neuroscience. New Orleans, LA. Oct. 25–30: 658.9.
- Hoang TQ, Ross BD, Bluml S, et al. 1998. Viability and neural proliferation in human fetal tissue transplants. *Proceedings of the 6th International Society for Magnetic Resonance in Medicine*. Sydney, Australia, April 18–24:483.
- Hope PL, Costello AM, Cady EB, Delpy DT, Tofts PS, Chu A, Hamilton PA, Reynolds EO, Wilkie DR. 1984. Cerebral energy metabolism studied with phosphorus NMR spectroscopy in normal and birth-asphyxiated infants. *Lancet* 2:366–370.
- Hossman K-A. 1994. Viability thresholds and the penumbra of focal ischemia. *Ann Neurol* 36:557–565.
- Hurd RE, Gurr D, Sailasuta N. 1998. Proton spectroscopy without water suppression: the oversampled J-Resolved experiment. *Magn Res Med* 40:343–347.
- Kanamori K, Ross BD. 1997. In vivo nitrogen MRS studies of rat brain metabolism. In: Bachelard H, editor. *Advances in neurochemistry*, Vol. 8. New York: Plenum Publishing. p 66–90.
- Kreis R. 1997. Quantitative localized ^1H MR spectroscopy for clinical use. *Prog Nucl Magn Reson Spectrosc* 31:155–195.
- Kreis R, Ernst T, Ross BD. 1993a. Absolute quantitation of water and metabolites in the human brain. Part II: metabolite concentrations. *J Magn Reson* 102:9–19.
- Kreis R, Ernst T, Ross BD. 1993b. Development of the human brain: in vivo quantification of metabolite and water content with proton magnetic resonance spectroscopy. *Magn Reson Med* 30:1–14.
- Kreis R, Farrow NA, Ross BD. 1990. Diagnosis of hepatic encephalopathy by proton magnetic resonance spectroscopy. *Lancet* 336:635–636.
- Kreis R, Farrow NA, Ross BD. 1991. Localized ^1H NMR spectroscopy in patients with chronic hepatic encephalopathy. Analysis of changes in cerebral glutamine, choline and inositols. *NMR Biomed* 4:109–116.
- Kreis R, Ross BD, Farrow NA, Ackerman Z. 1992. Metabolic disorders of the brain in chronic hepatic encephalopathy detected with ^1H MRS. *Radiology* 182:19–27.
- Kumar A, Welte D, Ernst RR. 1975. NMR Fourier zeugmatography. *J Magn Reson* 18:69–83.
- Mason GF, Gruetter R, Rothman DL, Behar KL, Shulman RG, Novotny EJ. 1995. NMR determination of the TCA cycle rate and α -ketoglutarate/glutamate exchange rate in rat brain. *J Cereb Blood Flow Metab* 15:12–25.
- Merboldt K-D, Bruhn H, Hanicke W, Michaelis T, Frahm J. 1992. Decrease of glucose in the human visual cortex during photic stimulation. *Magn Reson Med* 25:187–194.
- Merboldt KD, Chien D, Hanicke W, Gyngell ML, Bruhn H, Frahm J. 1990. Localized ^{31}P NMR spectroscopy of the adult human brain in vivo using stimulated-echo (STEAM) sequences. *J Magn Reson* 89:343–361.
- Michaelis T, Merboldt K-D, Bruhn H, Hanicke W, Frahm J. 1993. Absolute concentrations of metabolites in the adult human brain in vivo: quantification of localized proton MR spectra. *Radiology* 187:219–227.
- Michaelis T, Merboldt K-D, Hanicke W, Gyngell ML, Bruhn H, Frahm J. 1991. On the identification of cerebral metabolites in localized ^1H NMR spectra of human brain in vivo. *NMR Biomed* 4:90–98.
- Moreno A, Ross B, Bluml S. 2001. Direct determination of NAA synthesis rate of human brain in vivo. *J Neurochem* (in press).
- Mori S, Barker PB. 1999. Diffusion magnetic resonance imaging: its principle and applications. *Anat Rec (New Anat)* 257:102–109.
- Narayana PA, Johnston D, Flamig DP. 1991. In vivo proton magnetic resonance spectroscopy studies of human brain. *Magn Reson Imag* 9:303–308.
- Oberhaensli RD, Hilton Jones D, Bore PJ, Hands LJ, Rampling RP, Radda GK. 1986. Biochemical investigation of human tumours in vivo with phosphorus-31 magnetic resonance spectroscopy. *Lancet* 2:8–11.
- Ordidge RJ, Bendall MR, Gordon RE, Connelly A. 1985. Volume selection for in vivo biological spectroscopy. In: Govil G, Khetrpal CL, Saran A, editors. *Magnetic resonance in biology and medicine*. New Delhi: Tata McGraw-Hill. p 387–397.
- Ordidge RJ, Connelly A, Lohman JAB. 1986. Image-selected in vivo spectroscopy (ISIS). A new technique for spatially selective NMR spectroscopy. *J Magn Reson* 66:283–294.
- Pettegrew JW, Minschew NJ, Cohen MM, Kopp SJ, Glonek T. 1984. P-31 NMR changes in Alzheimer and Huntington diseased brain. *Neurology* 34:281.
- Prichard JW, Alger JR, Behar KL, Petroff OAC, Shulman RG. 1983. Cerebral metabolic studies in vivo by ^{31}P NMR. *Proc Natl Acad Sci USA* 80:2748–2751.
- Provencher SW. 1993. Estimation of metabolite concentrations from localized in vivo proton NMR spectra. *Magn Reson Med* 30:672–679.
- Ross BD. 1979. Techniques for investigation of tissue metabolism. In: Kornberg HC, Metcalf JC, Northcote D, Pogson CI, Tipton KF, editors. *Techniques in metabolic research*, part I. Vol. B203. Elsevier. p 1–22.
- Ross BD, Bluml S, Cowan R, Danielsen ER, Farrow N, Gruetter R. 1997. In vivo magnetic resonance spectroscopy of human brain: the biophysical basis of dementia. *Biophys Chem* 68:161–172.
- Ross BD, Kreis R, Ernst T. 1992. Clinical tools for the 90's: magnetic resonance spectroscopy and metabolite imaging. *Eur J Radiol* 14:128–140.
- Ross BD, Narasimhan PT, Tropp J, Derby K. 1989. Amplification or obfuscation: is localization improving our clinical understanding of phosphorus metabolism? *NMR Biomed* 2:340–345.
- Ross BD, Radda GK, Gadian DG, Rucker G, Esiri M, Falconer-Smith JC. 1981. Examination of a case of suspected McArdle syndrome by ^{31}P nuclear magnetic resonance. *N Engl J Med* 304:1338–1342.
- Rothman DL, Petroff OAC, Behar KL, Mattson RH. 1993. Localized ^1H NMR measurements of γ -aminobutyric acid in human brain in vivo. *Proc Natl Acad Sci* 90:5662–5666.
- Ryner LN, Sorenson JA, Thomas MA. 1995. Localized 2D J-Resolved ^1H MR spectroscopy: strong coupling effects in vitro and in vivo. *Magn Reson Imag* 13: 853–869.
- Seymour K, Bluml S, Sutherland J, Sutherland W, Ross BD. 1998. Identification of cerebral acetone by ^1H MRS in patients with epilepsy, controlled by ketogenic diet. (submitted).
- Seymour KJ, Bluml S, Sutherland J, Sutherland W, Ross BS. 1999. Identification of cerebral acetone by ^1H MRS in patients with epilepsy controlled by ketogenic diet. *MAGMA* 8:33–42.
- Shen J, Novotny EJ, Rothman DL. 1998. In vivo lactate and β -hydroxybutyrate editing using a pure phase refocusing pulse train. *Proceedings of the 6th Interna-*

- tional Society for Magnetic Resonance in Medicine. Sydney, Australia: 1883.
- Stockler S, Hanefeld F, Frahm J. 1996. Creatine replacement therapy in guanidinoacetate methyltransferase deficiency, a novel inborn error of metabolism. *Lancet* 348:789–790.
- Tallan HH. 1957. Studies on the distribution of *N*-acetyl-L-aspartic acid in brain. *J Biol Chem* 224:41–45.
- Thulborn KR, Ackerman JJH. 1983. Absolute molar concentrations by NMR in inhomogeneous B1. A scheme for analysis of in vivo metabolites. *J Magn Reson* 55:357–371.
- Thulborn KR, du Boulay GH, Radda GK. 1981. Proceedings of the Xth International Symposium on Cerebral Blood Flow and Metabolism.
- Van der Knaap MS, Ross BD, Valk J. 1993. Uses of MR in inborn errors of metabolism. In: Kucharczyk J, Barkovich AJ, Moseley M, editors. *Magnetic resonance neuroimaging*. Boca Raton: CRC Press, Inc. p 245–318.
- Webb PG, Sailasuta N, Kohler S, Raidy T, Moats RA, Hurd RE. 1994. Automated single-voxel proton MRS: technical development and multisite verification. *Magn Reson Med* 31:365–373.
- Welch KMA. 1992. The imperatives of magnetic resonance for the acute stroke clinician (Plenary Lecture). 11th Society of Magnetic Resonance in Medicine. Berlin: 901.
- Young IR. 2000. *Methods in biomedical magnetic resonance imaging and spectroscopy*. New York: John Wiley and Sons.
- Zeineh MM, Engel SA, Thompson PM, Bookheimer SY. 2001. Unfolding the human hippocampus with high resolution structural and functional MRI. *Anat Rec (New Anat)* 265:111–120.

APPENDIX

Appendix: How to Make MR Spectroscopy Measurements

APPLIED MRS-SINGLE-VOXEL ¹H MRS

When expertly performed, quantitative MRS brain studies provide results with a variance between 5 and 10% across large populations of normal subjects. The variance in single subjects may be as little as $\pm 3\%$, although measurements of complex-coupled peaks do not achieve better than $\pm 10\text{--}15\%$. The single greatest variable is not, we believe, true biological or diet-imposed variability but inaccuracy in positioning the patients' head or the VOI of localized MRS.

Below the reader can find a few suggestions on how to set up single-voxel proton MRS on a clinical scanner. These suggestions are heavily biased by the authors' experience with a General Electric 1.5 T Signa scanner. Nevertheless, the following section may be useful for users on any system because the underlying principles are the same on any scanner. Focusing for the moment on ¹H MRS, simple protocols with fixed echo time (TE) and repetitive time (TR) are best embedded in "macros," to prevent acquisition errors and to rigorously standardize techniques that may be required for longitudinal studies over many years. STEAM 20 ms (MPI, Göttingen), STEAM 30 ms (HMRI, Pasadena) and PRESS 30 ms have been "safe" choices and can be recommended. STEAM (or PRESS) 135 ms and 270 ms (or more recently 144 ms and 288 ms) are satisfactory long-echo times. Short-echo times TE give the smallest T₂ losses and therefore the best signal-to-noise (S/N) ratio and also the smallest susceptibility to T₂ changes in pathology. Background signals,

however, may cause considerable baseline distortions at extremely short TEs. To ensure reliability and quality we recommend performing a test as described below for single-voxel proton MRS based on axial localizers.

IDENTIFYING THE VOLUME OF INTEREST (VOI)

A few simple *preparations* should be done before starting the examination. We recommend to obtain a film with axial T₁ weighted images and to try to

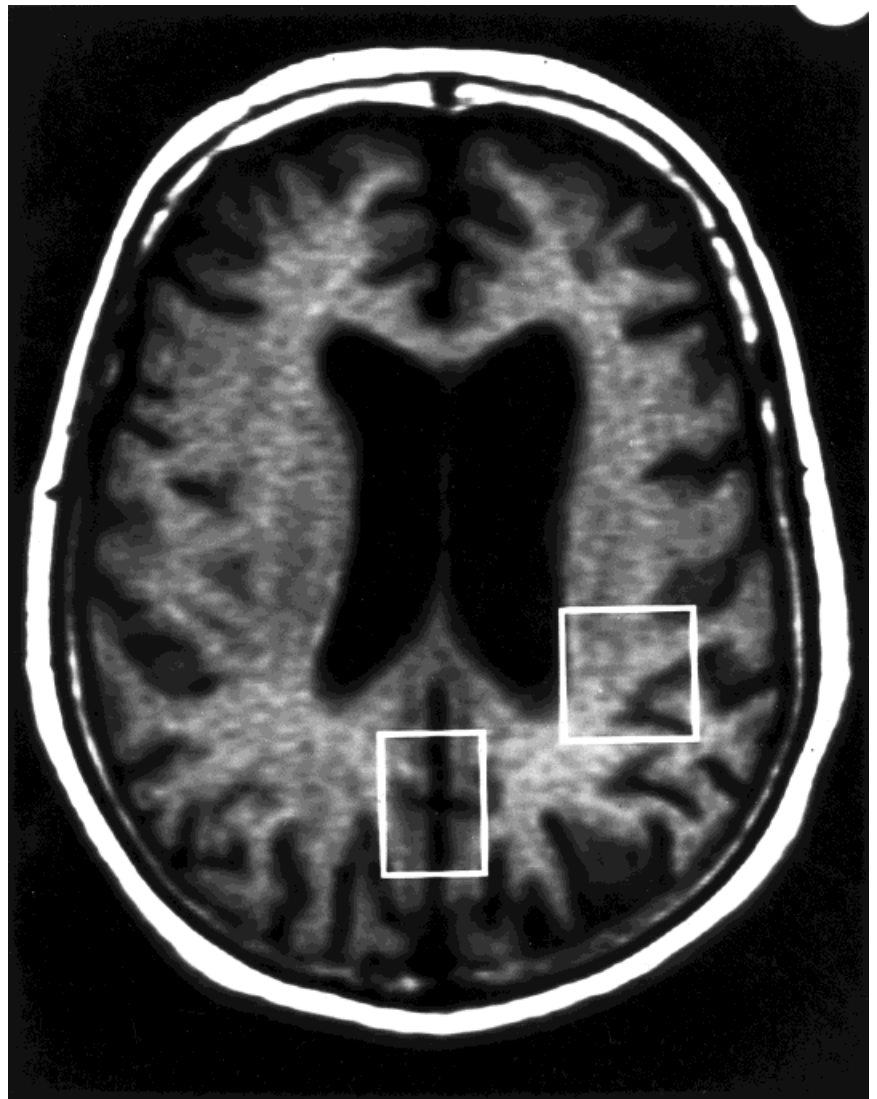


Figure 1S. MRI for voxel placement.

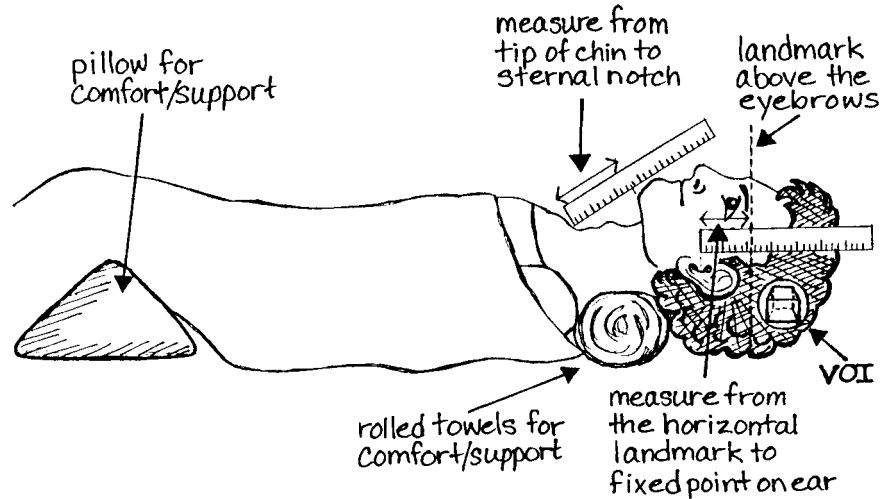


Figure 2S. Positioning subject for MRS of brain.

identify standard grey matter (GM) and white matter (WM) locations as used in the literature (see Fig. 1S and description below for HMRI definition). Mark the voxels with a pen on the film. Do the same on a set of T₂-weighted images. Accuracy in prescribing the voxel is of great importance! Remember, the slice thickness of an MRS voxel is typically 20 mm whereas the slice thickness of MRI is typically 5 mm. Therefore slices below and above the center slice for MRS need to be reviewed. Also check slices outside the range of the MRS voxel for being not too close to the skull. Con-

firm the voxel location with the following prescription:

Gray Matter

Center across falx at level 1 cm above posterior commissures of corpus callosum. Start inferior one slice (5 mm) above the slice with the a) internal capsule, b) angular artery in sylvian fissure, c) occipitoparietal fissure, d) vein of Galen, e) internal cerebral vein, f) frontal horn of lateral ventricle. Note: If the head is tilted not all of these landmarks may be visible. By choosing a voxel shape of 27 mm in A/P and 21 mm in R/L, most of the

tissue within the voxel is grey matter. The recommended slice thickness (S/I dimension) is 20 mm. Review above and below center position at least two slices (for 5 mm MRI slice thickness and 20 mm voxel slice thickness).

White Matter

Center left (or right) in parietal cortex. Stay in largely white matter, but allow up to 25% of grey matter. Landmarks are the center posterior rim of left (right) lateral ventricle ~1–1.5 cm above posterior commissures of corpus callosum. Review above two and

TABLE 1S. Locations for single-voxel MRS in various diseases

Diagnosis	Preferred location	Information needed
Global hypoxia Trauma	Gray matter Far away from blood/lesions. Gray matter (1st choice) to rule out hypoxic injury, white matter is 2nd choice. If there is no suspicion of hypoxic injury white matter is 1st choice.	Anticonvulsants? Conscious/unconscious Date of Injury?
Stroke (chronic) Liver disease; hepatic encephalopathy	Center (1st choice) and rim (2nd choice) Gray matter (1st choice), however earliest changes in liver disease are in white matter (2nd choice, Cho reduction)	Date of CVA Lactulose? Neomycin?
Dementia MS	Gray matter No evidence of lesions: White matter (1st choice). Lesions: Lesion (1st choice) and contra lateral side (2nd choice)	Clinical Dx? Symptoms?
HIV	Lesions: Lesion (1st choice), contra lateral side (2nd choice). No lesions: White matter	Medication, clinical diagnosis of lesion AIDS +, CD-4
HIV (AIDS dementia)	Through lesion/if no lesion gray matter: as above dementia	
Tumors, rule out tumors	Center of lesion suspicious region, sometimes smaller voxel necessary (adjust (increase) number of total scans); contralateral side as control. Repeat rim of lesion.	Type of tumor, chemo-, radiation therapy, Post-contrast o.k.
Unknown not focal disease	Gray matter	

NORMAL CONTROLS

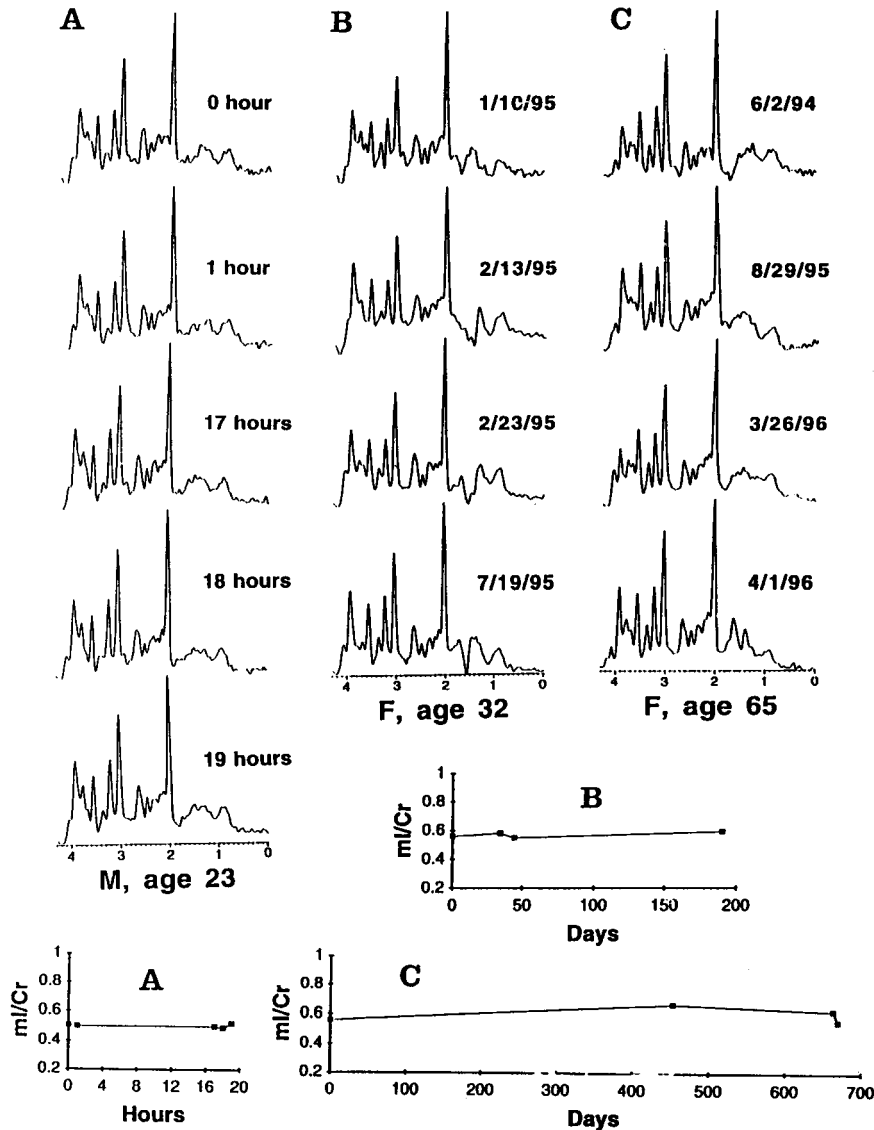


Figure 35. Stability and reproducibility of single-voxel MRS in controls and patients. Repeated single-voxel MRS (STEAM, TE = 30 ms, TR = 1.5 s, TM = 13.7 ms) in healthy controls and seventeen single-voxel MRS carried out in a patient with clinically suspected Alzheimer disease over a period of 13 months. All spectra can be distinguished from controls by elevated ml/Cr and reduced NAA/Cr, a feature of probable Alzheimer disease.

below at least two slices (for 5 mm MRI slice thickness and 20 mm voxel slice thickness). The S/I center position should be not more than 0–5 mm (superior) off from the grey matter center.

There is an element of subjectivity and “in-house” training in voxel placement. Landmarks are defined on the subject’s MRI. Voxel dimensions should be held constant for a given location. Here we encounter the first serious variable, which is the size of the head. Dimensions are tailored accordingly. Signal from outside the VOI is included in the final spectrum, because to the extent that pulse imperfections occur, the limits of the

VOI noted on the screen are inaccurate. The skilled spectroscopist avoids the worst problem, excess lipid signal, by selecting a VOI 5–7 mm away from the outer borders of the brain.

Finally, the best results should not depend on endless compliance of the subject. Protocols that include both MRI and MRS would do well to complete MRS and scout MRI if possible before, rather than after the bulk of the MRI protocol.

Subject Positioning

Plan the first tests at a time when there is no pressure for fast work. The subject is always supine. The RF head

coil center is always “landmarked” within 1 mm of the same position on the subjects’ head. The head is accurately positioned in all three planes. *Sagittal*: bore center at the mid-point of brow, nose and chin. *Coronal* (the commonest source of error) is selected only after defining the angle at which the subject is lying. Use a ruler to define the distance tip of chin to sternal notch and record this value for future MRS examinations. *Axial*: select a bony landmark, usually the supraorbital ridge, and drop a vertical through two other landmarks, say outer angle of the eye and tragus of the ear lobe (Fig. 2S). For even the most trivial procedure, it is recom-

PATIENT

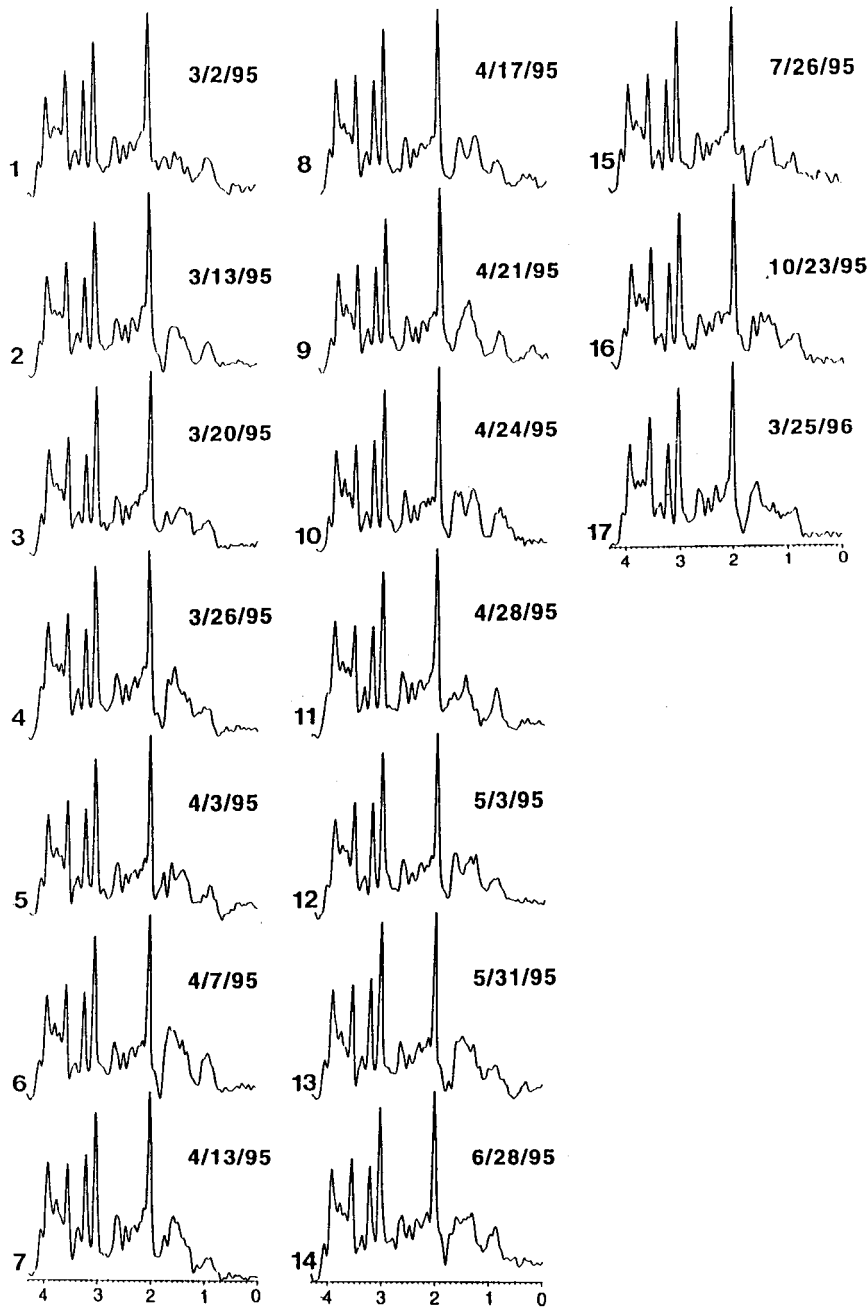


Figure 3S. (Continued)

mended that the head be fixed by Velcro straps. If an external reference is used for quantitation, it is important for automation and reproducibility that the vial is placed at the same position in all experiments.

Data Acquisition

Perform axial MRI and display image appropriate for center position. After

the scout MRI, angulation errors should be noted. Unless these are severe, the MRS can proceed.

MRS is prescribed in different ways on different instruments. They all have in common, however, the need to define coordinates orthogonal to the magnet bore (this explains the need to minimize angulation errors in initial positioning of the patient; they cannot

be accurately corrected despite the availability of all the desired landmarks on MRI).

Start with either a standard grey matter or white matter location. Do not forget how important it is to check the location in all slices covering the volume of interest (VOI). The MRI slice thickness is usually 5 mm, whereas the MRS slice thickness is 20 mm. Write down voxel position and voxel size.

The next step is the shimming and the adjustment of the scan parameters. A well-shimmed VOI is a prerequisite for good MRS, as resolution and lineshape have significant impact on the accuracy of the quantitation. Most scanners provide automated shimming that is generally faster than manual shimming and is the method of choice. Automated adjustment of RF transmitter gain, receiver gain, transmitter frequencies is standard on all modern scanners. Also the adjustment of the water suppression is automated on most systems. On a GE scanner using the PROBE™ (= PROton Brain Exam), all of the above steps are fully automated and can be done by pushing one button. Acquire the spectrum and print the spectrum or document it on a film. Save the spectrum file for later off-line processing.

Processing and Quantitation

Determine peak ratios and compare the spectrum with literature spectra. Stability and reproducibility are the key to successful longitudinal studies in neurophysiology and neuropathology. Figure 3S shows the results achieved in single subjects, volunteers and a patient with probable Alzheimer disease, illustrating the robustness of ^1H MRS over a 13-month period in normal and diseased human subjects. Dramatic neurochemical events, with a time constant of weeks or months, can also be readily observed (Ross and Michaelis, 1994). Two examples are shown in Figure 4S where ^1H MRS monitors the restoration of biochemical abnormalities after liver transplantation, and the appearance of ketone peak in the brain of a epileptic patient undergoing a ketogenic diet treatment (Seymour et al., 1999).

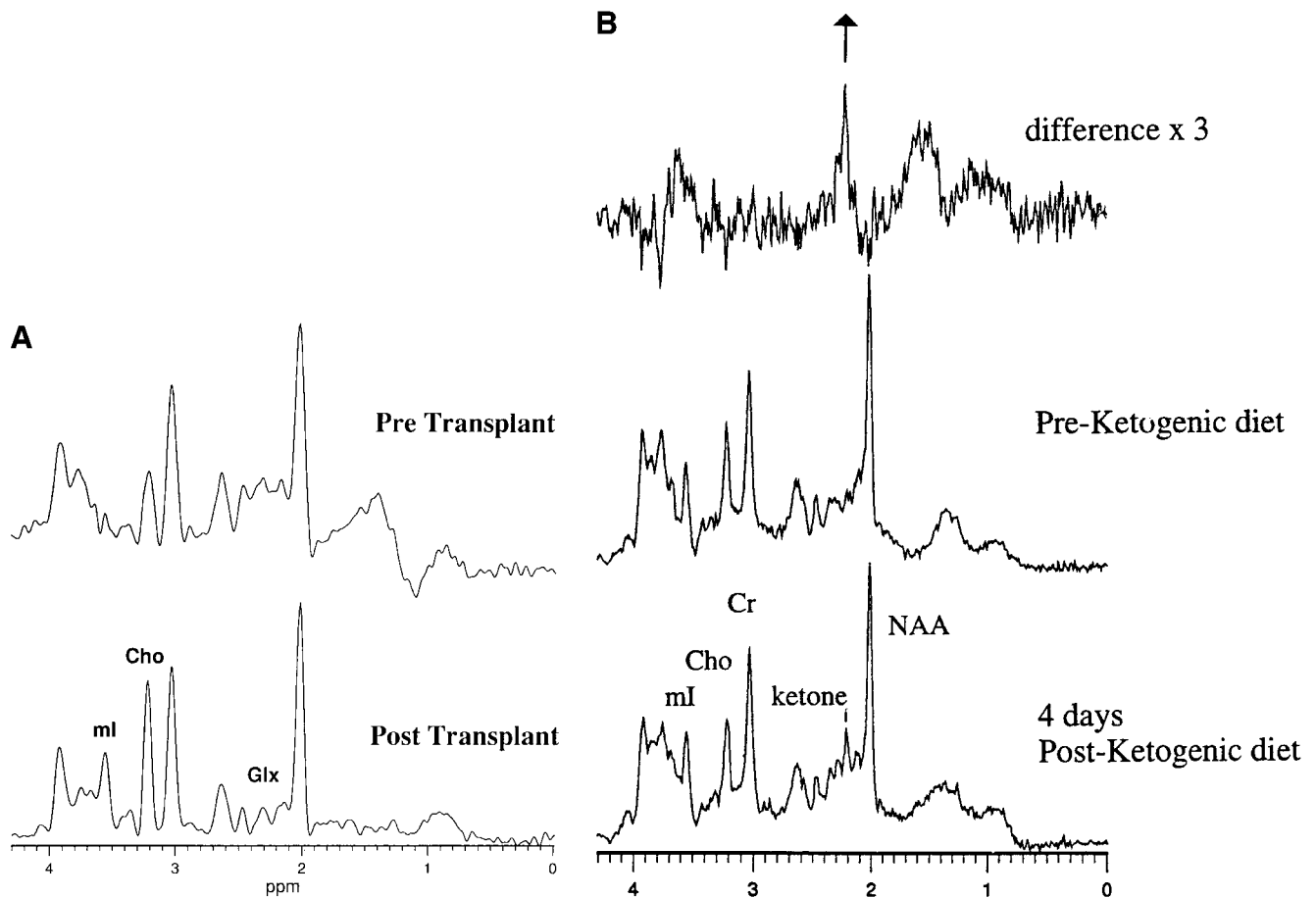


Figure 4S. The potential of MRS in diagnosis and treatment monitoring. **A:** Restoration of biochemical abnormalities of the brain post-liver transplant. The patient is a 30-year-old man with acute-on-chronic hepatic encephalopathy (HE) secondary to hepatitis and subsequently successfully treated by liver transplantation. Spectra were acquired 6 months apart from the same parietal white matter location, (15.0 cc stimulated-echo acquisition mode (STEAM) TR 1.5 s, TR 30 ms; NEX 128) and scaled to the same creatine (Cr) intensity for comparison. The obvious abnormalities before liver transplantation; increased α , β , and γ -glutamine; and reduced choline (Cho)/Cr and *myo*-inositol (ml)/Cr (upper spectrum) were completely reversed 3 months after transplantation and Cho/Cr exceeded normal (lower spectrum). **B:** Comparison of ^1H MRS in pre- and post-ketogenic diet in the same child. A ^1H MR spectrum from occipital grey matter of a patient before initiation of ketogenic diet reveals normal proton MRS (middle trace). Four days after starting the diet the ^1H spectrum acquired at the same location shows the presence of a single peak at 2.2 ppm (lower trace). The difference spectrum is shown in the upper trace (Seymour et al., 1999).

Where to Place the Voxel in Clinical Exams

The clinical question determines voxel location and size. In global diseases standard locations should be selected. The decision whether grey or white matter depends on the question asked. For example to predict outcome in head trauma, it is most important to rule out global hypoxic injury. For this question the grey matter location is more sensitive and would be the first choice. In tumors the voxel should be placed in the center of the

suspicious region minimizing partial volume with apparently normal tissue. In case of a small lesion two voxels at the same center position but with different volumes can be measured to estimate partial volume. There is some controversy about MRS after contrast agent. Because for short-echo time MRS in particular, there is no evidence for a significant impact of contrast agents on the spectral quality, the improved information about the region of interest after contrast agent may be favorable when MRI from a separate examination

with contrast agent is not available. For suggestions where to place the voxel in a clinical situation see Table 1S.

LITERATURE CITED

- Ross BD, Michaelis T. 1994. Clinical applications of magnetic resonance spectroscopy. *Magn Reson Quarterly* 10:191-247.
- Seymour, K, Bluml S, Sutherland J, Sutherland W, Ross BD. 1999. Identification of cerebral acetone by ^1H MRS in patients with epilepsy, controlled by ketogenic diet. *MAGMA* 8:33-34.